

EPJ D

Atomic, Molecular,
Optical and Plasma Physics

EPJ.org
your physics journal

Eur. Phys. J. D (2016) 70: 159

DOI: [10.1140/epjd/e2016-70195-4](https://doi.org/10.1140/epjd/e2016-70195-4)

On the thermodynamic properties of thermal plasma in the flame kernel of hydrocarbon/air premixed gases

Omid Askari, Gian Paolo Beretta, Kian Eisazadeh-Far and Hameed Metghalchi

edp sciences



 Springer

On the thermodynamic properties of thermal plasma in the flame kernel of hydrocarbon/air premixed gases

Omid Askari^{1,a}, Gian Paolo Beretta², Kian Eisazadeh-Far³, and Hameed Metghalchi¹

¹ Northeastern University, 334 Snell Engineering Center, 360 Huntington Ave, Boston, MA 02115-5000, USA

² Università di Brescia, Dipartimento di Ingegneria Meccanica e Industriale, via Branze 38, 25123 Brescia, Italy

³ Tula Technology, 2460 Zanker Rd, San Jose, CA, 95131, USA

Received 15 March 2016 / Received in final form 21 May 2016

Published online 2 August 2016 – © EDP Sciences, Società Italiana di Fisica, Springer-Verlag 2016

Abstract. Thermodynamic properties of hydrocarbon/air plasma mixtures at ultra-high temperatures must be precisely calculated due to important influence on the flame kernel formation and propagation in combusting flows and spark discharge applications. A new algorithm based on the complete chemical equilibrium assumption is developed to calculate the ultra-high temperature plasma composition and thermodynamic properties, including enthalpy, entropy, Gibbs free energy, specific heat at constant pressure, specific heat ratio, speed of sound, mean molar mass, and degree of ionization. The method is applied to compute the thermodynamic properties of H₂/air and CH₄/air plasma mixtures for different temperatures (1000–100 000 K), different pressures (10⁻⁶–100 atm), and different fuel/air equivalence ratios within flammability limit. In calculating the individual thermodynamic properties of the atomic species needed to compute the complete equilibrium composition, the Debye-Huckel cutoff criterion has been used for terminating the series expression of the electronic partition function so as to capture the reduction of the ionization potential due to pressure and the intense connection between the electronic partition function and the thermodynamic properties of the atomic species and the number of energy levels taken into account. Partition functions have been calculated using tabulated data for available atomic energy levels. The Rydberg and Ritz extrapolation and interpolation laws have been used for energy levels which are not observed. The calculated plasma properties are then presented as functions of temperature, pressure and equivalence ratio, in terms of a new set of thermodynamically self-consistent correlations that are shown to provide very accurate fits suitable for efficient use in CFD simulations. Comparisons with existing data for air plasma show excellent agreement.

1 Introduction

To improve efficiency and reduce pollutant formation in internal combustion engines [1], knowledge of flame kernel development and flame propagation play important role. A plasma, at very high temperature, will be generated at the onset of spark discharge. Accurate modeling of the thermodynamic properties of plasma mixtures is essential to understand the evolution of the plasma channel and its evolution into the formation of the flame kernel. During the spark discharge in a fuel-air mixture, the electrical energy is injected in a constant volume process followed by a sudden expansion which leads to the formation of fully ionized high temperature plasma through the generation of a shock wave and the consequent dissociation and ionization of the mixture. The plasma thermodynamic properties and its degree of ionization have important effects on flame ignition, structure, and propagation.

During the past decades a significant progress in plasma applications such as cutting, spraying, arc heating, re-entry of space-vehicles, nuclear rockets, CFD simulation of high-temperature flow fields and spark ignition has happened. To model and control the plasma flow in these applications, energy, mass, and momentum transfer are very important. As a result, the thermodynamic properties of plasma mixtures at high temperatures must be estimated by means of sophisticated models to ensure accurate simulations of the plasma flow field. In many applications it is possible to model plasma mixtures behavior by the equation of state of an ideal gas in local thermodynamic equilibrium (LTE).

In the last six decades, many papers have been published on the thermodynamic properties of plasma mixtures with particular attention to air species because of their importance in the aero-thermodynamic analysis of hypersonic flows surrounding a space vehicle during its reentry into the Earth's atmosphere. Gilmore [2,3] reported results for composition and thermodynamic properties of air for temperatures between 1000 K

^a e-mail: omidmech@gmail.com

and 24 000 K. Calculations assume a perfect gas mixture in local thermodynamic equilibrium, including dissociation and ionization. Hansen and Heims [4], and Hansen [5,6] studied the space-vehicle traveling at high speed which excite the air to high temperature, resulting in dissociation and ionization of air. His method was valid to predict the thermodynamic properties of air up to 15 000 K and considered dissociation and only first ionization of nitrogen and oxygen. Rosenbaum and Levitt [7] derived expressions for the composition, specific volume, enthalpy, and entropy of hydrogen plasmas up to 100 000 K.

Lick and Emmons [8] calculated the thermodynamic properties of helium plasmas at temperatures up to 50 000 K. They considered a mixture composed of neutral helium atoms, singly and doubly ionized helium atoms, and electrons. Brown calculated equilibrium high-temperature thermodynamic properties of the atmospheres of Earth [9], Mars [10] and Venus [11] for studying flights in planetary atmospheres in the shock and boundary layers. Drellishak et al. [12] calculated equilibrium composition and the thermodynamic properties of argon plasma for five pressures of 0.1, 0.5, 1.0, 2.0 and 5.0 atm, and for the temperature range from 5000 K to 35 000 K. Kubin and Presley [13] calculated the thermodynamic properties of hydrogen plasmas for a temperature up to 20 000 K. Hydrogen atoms were assumed to have only six energy levels. They neglected the reduction in the ionization potential and arbitrarily cut off the electronic partition function at six terms.

Patch and McBride [14] obtained thermodynamic properties for H_3^+ and H_2^+ at temperatures between 298 K and 10 000 K. Patch [15] calculated the equilibrium composition of a hydrogen plasma for pressures ranging from 1 to 100 atm at temperatures of 400 K to 40 000 K. Nelson [16] calculated and tabulated thermodynamic properties of an atomic hydrogen-helium plasma for temperatures from 10 000 K to 100 000 K. Pateyron et al. [17,18] calculated thermodynamic properties such as specific enthalpy and specific heat of the Ar- H_2 and Ar-He plasmas up to 30 000 K using partition functions of species. Sher et al. [19] calculated the specific heat capacity and mole fractions of the air at high temperatures using a simplified thermodynamic model to study the formation of spark channels. Capitelli et al. [20–24] calculated thermodynamic and transport properties of air at high temperatures assuming that the plasma is in local thermodynamic equilibrium (LTE) for temperatures up to 100 000 K. D'Angola et al. [25] calculated thermodynamic and transport properties of high temperature equilibrium air plasmas in a wide range of pressure (0.01 atm to 100 atm) and temperature range (50 to 60 000 K). Rat et al. [26] performed an alternate derivation of transport properties in a nonreactive two-temperature plasma without Bonnefoi's assumptions. They applied their model for a two-temperature argon plasma and figured that the theory of transport coefficients of Devoto and Bonnefoi underestimates the electron thermal conductivity. Murphy calculated the transport coefficients such as viscosity, thermal conductivity and electrical conductivity of different species including hydrogen and mixtures of

argon-hydrogen [27] and helium and its mixture with argon [28] using local thermodynamic equilibrium at atmospheric pressure in the temperature range from 300 to 3000 K.

The above literature shows that most of the works dealt only with air and some fundamental gases like, hydrogen, helium, argon, and their mixtures. It also reveals a shortage of exact curve-fit correlations of thermodynamic properties of fuel/air plasma mixtures such as hydrogen/air and methane/air which have many important applications in automotive and aviation industries [29,30], as well as in other studies dealing with plasma mixtures. The combustion community suffers from lack of these kind of correlations which in CFD simulations of plasma mixture flows can be easily implemented and effectively reduce numerical complications and computation time. Curve-fit correlations have only been reported in few works with high emphasis on air plasma.

The purpose of this paper is to provide the thermodynamic properties and equilibrium composition of hydrogen/air and methane/air plasma mixtures. The correlations we propose provide the equilibrium composition and the thermodynamic properties such as enthalpy, entropy, Gibbs free energy, specific heat at constant pressure, specific heat ratio, speed of sound, mean molar mass, and degree of ionization for a wide range of temperatures (1000–100 000 K), pressures (10^{-6} – 10^2 atm) and different equivalence ratios within flammability limit (for methane/air mixture flammability limit is $0.6 < \phi < 1.4$ and for hydrogen/air mixture flammability limit is $0.5 < \phi < 5.0$). To calculate the thermodynamic properties of a plasma mixture, it is necessary to evaluate the individual properties of the pure components and calculate the equilibrium composition. For polyatomic molecules and molecular ions, which are the dominant components during the dissociation phase, the individual thermodynamic properties are extracted from the NASA database [31]. For monoatomic molecules, atomic ions, and electrons, the individual thermodynamic properties are computed by statistical thermodynamic methods using a rigorous calculation of the electronic partition functions. Griem's self-consistent model [32] is used for the reduction of the ionization potential based on Debye-Huckel length. This model uses a cut-off of the electronic partition function expansion series in order to prevent its divergence problem. The effect of the number of energy levels on thermodynamic properties is illustrated by comparing the results with the ground state method. In order to determine the equilibrium composition, the complete equilibrium method based on Gibbs free energy minimization assuming ideal gas equation of state, mass conservation, and electrical neutrality [33,34] has been applied.

The paper is structured as follows. Section 2 discusses the importance of plasma study in flame kernel modeling in the spark ignition process. Section 3 illustrates the model and the various assumptions in detail. Section 4 presents and discusses the results. Section 5 gives some conclusions. Appendix gives the coefficients of the proposed correlations.

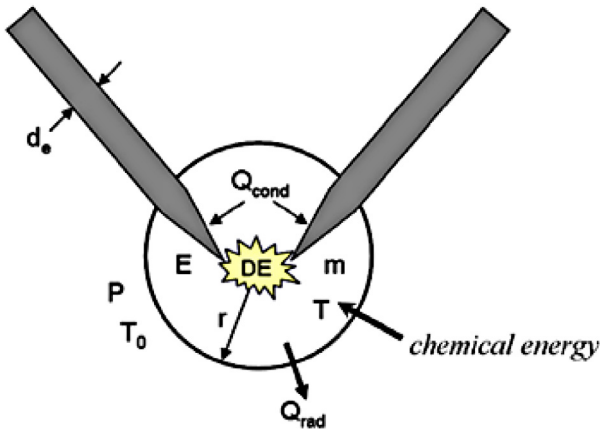


Fig. 1. Schematic of flame propagation model [35].

2 Plasma application in spark ignition process

It is a well-known fact that in the spark and laser ignition, high temperature ionized gases is the source of flame kernel formation and propagation. In conventional spark ignition, electrical energy is supplied through an external source (e.g. a spark plug). A part of electrical energy is converted to thermal energy by ionizing the gases. This conversion process involves the formation of a plasma kernel which can potentially form a flame kernel. The formation of spark kernel consists of two parts [35]. The first, the shorter stage involves a pressure wave emission; the second stage which is longer is a constant pressure process. In the second stage the diffusion of reactants and ions conclude the initial flame kernel [35]. In both stages the high density electrical energy creates ions in an extremely high temperature environment. In our previous work, we calculated the properties of the initial spark kernel by employing a thermodynamic model validated by experiments [35]. For an initial plasma kernel the energy balance for the control volume shown in Figure 1, is given by:

$$\frac{\partial E}{\partial t} = \dot{m}_b (h_{u_f} + c_{p_u} T_u) + \frac{dSE}{dt} - \dot{Q}_{cond} - \dot{Q}_{rad} - P\dot{V}, \quad (1)$$

$$E = m (u_{b_f} + c_{v_b} T_b), \quad (2)$$

where E is the energy of the burned gas region, m the mass of the gas, T the temperature, h the specific enthalpy, u the specific internal energy, c_p the specific heat at constant pressure, c_v the specific heat at constant volume, SE the supplied spark energy, t the time, Q_{cond} the conductive energy losses, Q_{rad} the radiated energy losses, P the pressure and V the volume of the kernel, u, b and f subscripts refer to unburned, burned and formation.

By solving equations (1) and (2), the kernel temperature at several conditions was calculated. Figure 2 shows the temperature of kernel at different initial radii. It can be seen that the temperature is high enough for the formation of plasma ions. We have shown that at temperatures higher than 6000 K the thermodynamic properties such as c_v and c_p in equations (1) and (2) are strong

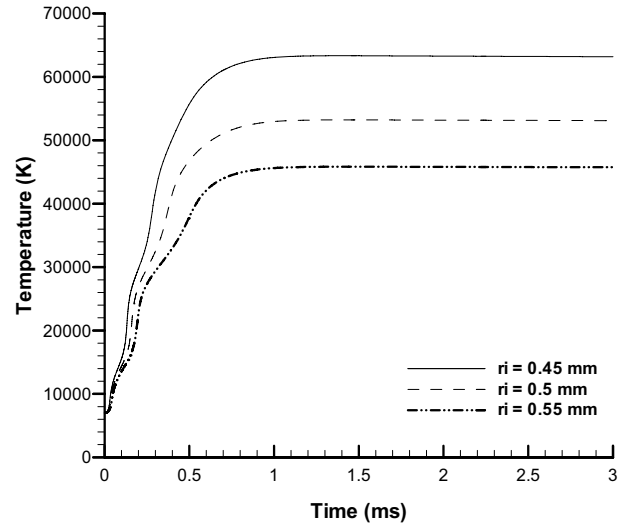


Fig. 2. The effect of initial radius on air kernel temperature, $T_i = 7000$ K, discharge energy = 24 mJ [35].

function of ionization processes [36]. In previous work [35] due to low concentration of methane molecule the thermodynamic properties of methane/air plasma were approximated by considering only air and neglecting methane in the mixture. This rough assumption can be resolved by keeping all the components available in the real plasma mixture which will enhance the accuracy of thermodynamic properties by including hydrogen, helium, carbon, argon and neon ions in the computations. Laminar burning speed [37–40], an important thermo-physical properties of combustible mixtures, can be calculated using the method introduced in previous publication [35] in conjunction with exact plasma simulation of hydrocarbon/air pre-mixed gases in this study at ultra-high pressures at which the flame is always cellular and unstable.

3 Method of calculation

The calculations described here, and the resulting correlations, are based on the following three assumptions, which are valid for many plasma mixtures: (1) the plasma is in local thermodynamic equilibrium; (2) the plasma mixture is quasi-neutral; and (3) the plasma mixture and its individual components obey the ideal gas equation of state. Under such conditions, Boltzmann statistics is applicable. Calculations have been carried out in two different temperature ranges, called dissociation and ionization. To obtain realistic calculations, all minor species have been considered, for an overall of 133 species as listed in Table 1 for both methane/air and hydrogen/air plasma mixtures.

3.1 Dissociation temperature range

Increasing the temperature of a gas mixture causes the molecules not only to vibrate but also to dissociate into elemental atoms. Depending on the initial gas mixture composition the dissociation temperature range is typically

Table 1. List of the 133 species considered in the present calculations for H₂/Air and CH₄/Air plasma mixtures.

Plasma mixture	Available species
H ₂ /Air and CH ₄ /Air ¹ [41]	CH, CH ⁺ , CH ₂ , CH ₂ OH, CH ₂ OH ⁺ , CH ₃ CH ₃ O, CH ₃ OHCH ₄ , C ₂ H, C ₂ H ₂ , CH ₂ CO, C ₂ H ₃ , CH ₃ CN, CH ₃ CO, C ₂ H ₄ , C ₂ H ₄ O, CH ₃ CHO, C ₂ H ₅ , C ₂ H ₆ , C ₃ H ₇ , C ₃ H ₈ , CN, CN ⁺ CN ⁻ , CNN, CO, CO ⁺ , CO ₂ , CO ₂ ⁺ NCO, HCO, HCO ⁺ , HCN, HCCN, HCCO, HNC, HNCO, HNO, OH, OH ⁻ OH ⁺ , HO ₂ , HO ₂ ⁻ , H ₂ O, H ₂ O ⁺ , H ₂ O ₂ , NH, NH ⁺ , NH ₂ , NH ₃ , NO, NO ⁺ NO ₂ , NO ₂ ⁻ , N ₂ ON ₂ O ⁺ H ₂ , H ₂ ⁻ , H ₂ ⁺ , H, H ⁻ , H ⁺ He, He ⁺ , He ⁺² , C, C ⁻ , C ₂ , C ₂ ⁻ C ₂ ⁺ , C ⁺ , C ⁺² , C ⁺³ , C ⁺⁴ , C ⁺⁵ , C ⁺⁶ N, N ⁻ , N ₂ , N ₂ ⁻ , N ₂ ⁺ , N ⁺ , N ⁺² , N ⁺³ , N ⁺⁴ , N ⁺⁵ , N ⁺⁶ , N ⁺⁷ , O, O ⁻ , O ₂ , O ₂ ⁻ , O ₂ ⁺ , O ⁺ O ⁺² , O ⁺³ , O ⁺⁴ O ⁺⁵ , O ⁺⁶ , O ⁺⁷ , O ⁺⁸ , Ne, Ne ⁺ , Ne ⁺² , Ne ⁺³ , Ne ⁺⁴ , Ne ⁺⁵ , Ne ⁺⁶ , Ne ⁺⁷ Ne ⁺⁸ , Ne ⁺⁹ , N ⁺¹⁰ Ar, Ar ⁺ , Ar ⁺² , Ar ⁺³ , Ar ⁺⁴ , Ar ⁺⁵ Ar ⁺⁶ , Ar ⁺⁷ , Ar ⁺⁸ , Ar ⁺⁹ , Ar ⁺¹⁰ , Ar ⁺¹¹ , Ar ⁺¹² , Ar ⁺¹³ , Ar ⁺¹⁴ , Ar ⁺¹⁵ Ar ⁺¹⁶ , Ar ⁺¹⁷ , Ar ⁺¹⁸ , e ⁻

¹ N₂: 78.084%, O₂: 20.946, Ar: 0.9335%, CO₂: 0.03398%, Ne: 0.001818% and He: 0.000702%.

characterized by lots of chemical reactions all actively contributing to determine the equilibrium composition. Under such conditions, the accurate approach to compute the equilibrium composition for given temperature and pressure is a complete equilibrium calculation [42], namely, Gibbs free energy minimization constrained by elemental conservation and electrical neutrality. The minimization algorithm used here is based on Lagrange's multipliers as implemented in the RAND method [33,34]. The thermodynamic properties for the molecules and molecular ions are taken from NASA database [31] up to 20 000 K.

3.2 Ionization temperature range

At even higher temperatures the gas mixture is characterized by the formation of positively charged ions and unbound electrons created by the ionization reactions. Ions and electrons have a significant effect on plasma properties at high temperatures and because of that a rigorous statistical model which is described in the following sections has been developed.

3.2.1 Thermodynamic properties of individual monoatomic species

The important step in calculating the high temperature properties of plasma mixtures is to calculate the pure-substance thermodynamic properties of the individual monoatomic species participating in the ionization reactions, i.e., neutral atoms, positive atomic ions, and electrons. For gaseous species the thermodynamic functions may be calculated from spectroscopic constants using the partition function concept [43]. Using the statistical thermodynamics formulation, the partition functions and their first and second derivatives discussed in detail in Section 3.2.2, we can compute all the pure-substance thermodynamic properties. The specific enthalpy (kJ/kg) and specific entropy (kJ/kg K) of the pure *i*th species are given

respectively by

$$h_{ii}(T, P) = 2.5 \frac{\bar{R}T}{M_i} + \frac{\bar{R}T^2}{M_i} \frac{1}{Q_{e_i}^*} \frac{\partial Q_{e_i}^*}{\partial T}, \quad (3)$$

$$s_{ii}(T, P) = 2.5 \frac{\bar{R}}{M_i} + \frac{\bar{R}T}{M_i} \frac{1}{Q_{e_i}^*} \frac{\partial Q_{e_i}^*}{\partial T} + \frac{\bar{R}}{M_i} \ln \left[Q_{e_i}^* \left(\frac{2\pi M_i}{N_A} \right)^{3/2} (kT)^{5/2} h_p^{-3} P^{-1} \right] \quad (4)$$

where, following reference [42] the double subscript *ii* in h_{ii} and s_{ii} is used to denote pure-substance specific properties, and to distinguish them from the partial properties h_i and s_i of the same component in the mixture; moreover,

$$Q_{e_i}^* = Q_{e_i} e^{\frac{-\epsilon_i^*}{kT}} \quad (5)$$

$$\frac{\partial Q_{e_i}^*}{\partial T} = \left[\frac{\partial Q_{e_i}}{\partial T} + \frac{Q_{e_i}}{kT^2} \left(\epsilon_i^* - T \frac{\partial \epsilon_i^*}{\partial T} \right) \right] e^{\frac{-\epsilon_i^*}{kT}} \quad (6)$$

where ϵ_i^* is the energy of formation of the *i*th species, Q_{e_i} is the electronic partition function of the *i*th species, M_i is its molar mass, \bar{R} the universal gas constant, N_A Avogadro's number, k the Boltzmann constant, h_p the Planck constant, P the pressure and T the gas temperature. The pure-substance specific Gibbs free energy (kJ/kg) is calculated from enthalpy and entropy, $g_{ii} = h_{ii} - T s_{ii}$, i.e.,

$$g_{ii}(T, P) = \mu_{ii}(T, P) = \frac{\bar{R}}{kM_i} \left(\epsilon_i^* - T \frac{\partial \epsilon_i^*}{\partial T} \right) - \frac{\bar{R}T}{M_i} \ln \left[Q_{e_i}^* \left(\frac{2\pi M_i}{N_A} \right)^{3/2} (kT)^{5/2} h_p^{-3} P^{-1} \right] \quad (7)$$

where the first equality is a reminder that for the pure substance the specific Gibbs free energy is equal to the chemical potential. The pure-substance specific heat at constant pressure is evaluated as the partial derivative

of the specific enthalpy with respect to temperature,

$$c_{p_{ii}}(T, P) = 2.5 \frac{\bar{R}}{M_i} + 2 \frac{\bar{R}T}{M_i} \frac{1}{Q_{e_i}^*} \frac{\partial Q_{e_i}^*}{\partial T} - \frac{\bar{R}T^2}{M_i} \left(\frac{1}{Q_{e_i}^*} \right)^2 \left(\frac{\partial Q_{e_i}^*}{\partial T} \right)^2 + \frac{\bar{R}T^2}{M_i} \frac{1}{Q_{e_i}^*} \frac{\partial^2 Q_{e_i}^*}{\partial T^2}, \quad (8)$$

where

$$\begin{aligned} \frac{\partial^2 Q_{e_i}^*}{\partial T^2} = & \left[\frac{\partial^2 Q_{e_i}}{\partial T^2} + \frac{2}{kT^2} \left(\epsilon_i^* - T \frac{\partial \epsilon_i^*}{\partial T} \right) \frac{\partial Q_{e_i}}{\partial T} \right. \\ & + \frac{1}{k^2 T^4} \left(\epsilon_i^* - T \frac{\partial \epsilon_i^*}{\partial T} \right)^2 Q_{e_i} \\ & \left. - \frac{2}{kT^3} \left(\epsilon_i^* - T \frac{\partial \epsilon_i^*}{\partial T} \right) Q_{e_i} - \frac{1}{kT} \frac{\partial^2 \epsilon_i^*}{\partial T^2} Q_{e_i} \right] e^{-\frac{\epsilon_i^*}{kT}} \end{aligned} \quad (9)$$

and we note that, differently from the standard ideal gas model, the enthalpy and the specific heat here depend, though slightly, on pressure through the pressure-dependent cut-off criterion that we adopt for the electronic partition function, as explained in the next section.

3.2.2 Partition function

To calculate the pure-substance thermodynamic properties and the equilibrium mass fractions of all the species present in the plasma, the knowledge of partition functions and their derivatives are prerequisites. In general, the partition function of a molecular system can be expressed by translational and internal contributions

$$Q = Q_{tr} Q_{int}. \quad (10)$$

The internal contribution may be due to the rotational, vibrational, and electronic motions within the particle ($Q_{int} = Q_r Q_v Q_e$). For an atomic system (atoms, atomic ions and electrons) the rotational and vibrational partition functions take the value of unity, so translational and electronic partition functions for such species are:

$$Q_{tr} = \left(\frac{2\pi m k T}{h_p^2} \right)^{3/2} \frac{\bar{R}T}{P} \quad (11)$$

$$Q_e = \sum_n g_n e^{-\frac{\epsilon_n}{kT}} = \sum_n (2J_n + 1) e^{-\frac{\epsilon_n}{kT}} \quad (12)$$

where m is the mass of the molecule, ϵ_n is the electronic energy of the n th level of the species under consideration, g_n its statistical weight, and J_n the corresponding angular momentum quantum number.

However, the summation in equation (12) diverges because the statistical weight increases rapidly with the number of energy levels (e.g., for hydrogen atoms, $g_n \propto n^2$). This behavior is correct just for a hypothetical isolated atomic species, while interactions with other species in the plasma mixture limit the number of energy levels. So an appropriate *cut-off criterion* is required for the termination of electronic partition function of atomic species to define an upper limit for the aforementioned series.

3.2.2.1 Cut-off criteria

The only problem to calculate the pure-substance thermodynamic properties of plasma mixtures is that the series for the electronic partition function of atomic species does not have an upper bound. The exponential terms in equation (12) approach a finite limit corresponding to the ionization potential, which is the upper bound to the energy but the statistical weight increases as the square of the number of energy levels and consequently the series diverges. On the other hand, it has been observed experimentally that as the temperature increases, due to a polarizing effect of neighboring charged particles, the ionization potential of particles in a plasma is lowered [44]. In order to prevent numerical divergence and match the empirically observed lowering of the ionization potential, a criterion is needed for terminating the series of the electronic partition function. A review of various cut-off criteria can be found in reference [45,46]. These cut-off criteria may be summarized as the following types:

1. no dependence on temperature or pressure [46,47];
2. dependence on temperature only [46,48];
3. dependence on temperature and pressure (or number density) [12,32].

The ionization potential of an atomic species in the presence of other ions and electrons is decreased due to the action of the Coulomb fields. This reduction depends on the number densities of the charged particles or the gas pressure. This means that the pure-substance thermodynamic properties of single atomic species in the ionization range depend on both temperature and pressure. The well-known Griem model [32,49] adopts the cut-off criterion to include only energy levels below reduced ionization potential,

$$\epsilon_n \leq IP - \Delta IP. \quad (13)$$

In current work the observed energy levels reported by Moore [50] and NIST¹ have been completed with the Rydberg-Ritz formulas using the isoelectronic sequence method [51]. For the atomic species including only one electron which are called hydrogenic species (H^+ , He^+ , C^{+6} , N^{+7} , O^{+8} , ...) the statistical weight (g_n) and energy (ϵ_n) of n th level have been evaluated using the following relations,

$$g_n = 2n^2, \quad (14)$$

$$\epsilon_n = IP \left(1 - \frac{1}{n^2} \right). \quad (15)$$

3.2.2.2 Reduced ionization potential

The reduced ionization potential, ΔIP adopted by the Griem model [32,49] depends on the plasma composition via the Debye-Huckel length l_D and by making a self-consistent solution for the problem. The reduction of the ionization potential of an atomic specie of charge z is

$$\Delta IP_i = \frac{(z_i + 1) e^2}{l_D}, \quad (16)$$

¹ <http://www.nist.gov/pml/data/asd.cfm> (2015).

where the Debye length is defined as

$$l_D = \left[\frac{kT}{4\pi e^2 \left(\sum_{i=1}^{NS} N_i z_i^2 \right)} \right]^{1/2}, \quad (17)$$

where e is the charge of an electron, NS is the number of all species present in the plasma including electrons and N_i is the number density of i th species. Equation (16) applies for densities and temperatures for which the Debye theory is valid. Griem [32] and Cooper [52] derive the criterion for the validity of the Debye theory as

$$\sum_{i=1}^{NS} N_i \geq \frac{1}{8\pi l_D^3}. \quad (18)$$

3.2.3 Complete equilibrium solution based on Gibbs free energy minimization

This method is based on Gibbs free energy minimization under the assumption of Gibbs-Dalton mixture of ideal gases [42] and subject to the constraints of element conservation and electrical neutrality [33,34]. To determine complete equilibrium composition at a given temperature and pressure, the Gibbs free energy of the mixture must be minimized, subject only to the constraints of element conservation, electrical neutrality, and non-negativity of the mole numbers, i.e.,

$$\begin{cases} \sum_{i=1}^{NS} a_{ij} n_i = q_j n_{C_k H_l} \quad j = 1, \dots, m \\ \sum_{i=1}^{NS} a_{i0} n_i = 0 \\ n_i \geq 0 \quad \forall i \end{cases} \quad (19)$$

where $n_{C_k H_l}$ is the mole number of hydrocarbon $C_k H_l$ in the initial fuel-air mixture, n_i is the mole number of species i in the equilibrium plasma mixture, NS the number of species present in the plasma mixture, m the number of different elements, a_{ij} represents the number of elements of type j that compose the atom or molecule of species i so that q_j (dimensionless) represents the (fixed) number of elements of type j in the mixture per unit mole number of hydrocarbon in the initial fuel-air mixture, and a_{i0} represents the electrical charge of species i . In what follows we will denote by \mathbf{q} the vector q_1, \dots, q_m of the given amounts of the elements in the mixture per unit amount of initial fuel. For an initial $C_k H_l$ -air mixture with equivalence ratio ϕ and molar composition of air given by $x_{N_2}^a N_2 + x_{O_2}^a O_2 + x_{H_2O}^a H_2O + x_{Ar}^a Ar + x_{CO_2}^a CO_2 + x_{Ne}^a Ne + x_{He}^a He$ the values of the q_j 's are listed in Table A.1 in Appendix.

Under the assumption of Gibbs-Dalton mixture of ideal gases, the Gibbs free energy of the reacting mixture at a generic non-equilibrium composition can be

written as:

$$\begin{aligned} G(T, P, \{n_i\}) &= \sum_{i=1}^{NS} n_i \mu_{i,\text{off}}(T, P, \{n_i\}) \\ &= \sum_{i=1}^{NS} n_i \left[\mu_{ii}^0(T) + RT \ln \left(\frac{n_i}{\sum_{j=1}^{NS} n_j} \right) \right. \\ &\quad \left. + RT \ln \left(\frac{P}{P^0} \right) \right], \end{aligned} \quad (20)$$

where, following [42], $\mu_{i,\text{off}}(T, P, \{n_i\})$ denotes the chemical potential of species i in the so-called ‘‘surrogate system’’, namely, the frozen-composition non-reacting mixture (hence the ‘‘off’’ subscript) at stable equilibrium with the same temperature T , pressure P , and composition $\{n_i\}$ as the actual non-equilibrium state of the reacting mixture, and μ_{ii}^0 is the chemical potential of pure species i at temperature T and the standard pressure $P^0 = 1$ atm, which we have defined in terms of partition functions in the preceding section.

The minimization is done using an equilibrium composition solver based on the well-known algorithm developed in reference [34] and convergence is considered satisfied based on the following condition:

$$\frac{\Delta n_i}{n_i} < 10^{-15} \quad \forall i. \quad (21)$$

As shown in reference [42], the solution can be formally expressed in terms of a set of $m + 1$ Lagrange multipliers $\lambda_j(T, P, \mathbf{q})$, with $j = 0, 1, \dots, m$, so that the complete-equilibrium mole fractions are given by

$$x_i(T, P, \mathbf{q}) = \frac{P^0}{P} \exp \left[\frac{1}{R} \sum_{j=0}^m \lambda_j(T, P, \mathbf{q}) a_{ij} - \frac{1}{RT} \mu_{ii}^0(T) \right]. \quad (22)$$

Once the mole fractions x_i are obtained, the mass fractions are readily found from $y_i(T, P, \mathbf{q}) = x_i M_i / \sum_k x_k M_k$.

3.2.3.1 Iterative solution

The iterative solution to find the mole fractions of all species at a given temperature, pressure, and elemental composition proceeds as follows. Using the last calculated mole fractions, we estimate the number densities N_i using the ideal gas law

$$N_i(T, P, \mathbf{q}) = \frac{n_i}{V} = \frac{n_i}{n} \frac{P}{RT} = x_i(T, P, \mathbf{q}) \frac{P}{RT} \quad (23)$$

to evaluate (i) the Debye length; (ii) the lowered ionization potential; and (iii) the maximum number of energy levels based on the cut-off criterion. Then the partition function is calculated by summing over all such energy

levels. The species mole fractions are then re-calculated using these partition functions and the equilibrium composition solver. The new mole fractions are then used and a new Debye length is determined. In general, the previous value of the Debye length and the new calculated value do not agree. Therefore, the new value is used to compute again an improved partition function, and the process is repeated until convergence is reached on the value of the Debye length.

3.3 Mixture thermodynamic properties

Once the complete-chemical-equilibrium mole fractions of all the species are obtained, the (mass) specific properties of the plasma mixture are determined using the Gibbs-Dalton mixture model. Showing explicitly all dependences, we have

$$h(T, P, \mathbf{q}) = \sum_{i=1}^{NS} y_i(T, P, \mathbf{q}) h_{ii}(T, P) \quad (24)$$

$$s(T, P, \mathbf{q}) = \sum_{i=1}^{NS} y_i(T, P, \mathbf{q}) \times \left(s_{ii}(T, P) - \frac{\bar{R}}{M_i} \ln(x_i(T, P, \mathbf{q})) \right) \quad (25)$$

$$g(T, P, \mathbf{q}) = h(T, P, \mathbf{q}) - Ts(T, P, \mathbf{q}). \quad (26)$$

The mean molar mass is calculated as

$$M_t(T, P, \mathbf{q}) = \left[\sum_{i=1}^{NS} \frac{y_i(T, P, \mathbf{q})}{M_i} \right]^{-1} \quad (27)$$

The mass specific gas constant is

$$R(T, P, \mathbf{q}) = \frac{\bar{R}}{M_t(T, P, \mathbf{q})}. \quad (28)$$

The density and the mass specific volume $v(T, P, \mathbf{q}) = 1/\rho(T, P, \mathbf{q})$ can be obtained from the relation

$$\rho(T, P, \mathbf{q}) \cong \frac{M_t(T, P, \mathbf{q}) P}{\bar{R}T} \quad (29)$$

and therefore the (mass) specific internal energy is given by:

$$u(T, P, \mathbf{q}) = \sum_{i=1}^{NS} y_i(T, P, \mathbf{q}) u_{ii}(T, P) \cong h(T, P, \mathbf{q}) - \frac{\bar{R}T}{M_t(T, P, \mathbf{q})}. \quad (30)$$

In the last two relations we use the 'approximately equal to' symbol because the electronic partition functions depend (slightly) on pressure through the cut-off criterion, and therefore neither the individual species nor the mixture strictly obey the ideal gas equations of state. However, we have verified that the departure is essentially negligible for all species. The specific heat for oxygen atom

and its ions versus temperature for three different pressures of 10^{-6} , 1 and 100 atm are plotted in Figure 3. As it is obvious, the effect of pressure is very negligible especially for the ions, which are the main species at high temperatures.

To compute specific heats at constant pressure and volume, $c_{p,\text{off}}$ and $c_{v,\text{off}}$, the specific heat ratio γ_{off} , the isentropic exponent $\gamma_{s,\text{off}}$, and the speed of sound χ_{off} , we must recall that according to the standard model of chemical kinetics (again, for a fully explicit discussion see [42]) these properties are generally defined at arbitrary compositions in terms of the so-called "surrogate system". Here, the plasma composition is that of complete chemical equilibrium, hence the surrogate system is the frozen-composition, non-reacting mixture at stable equilibrium with the given temperature T and pressure P , and the (fixed) composition (T, P, \mathbf{q}) . Therefore, the partial derivatives with respect to temperature must be evaluated keeping the γ_i 's fixed, so that we have

$$c_{p,\text{off}}(T, P, \mathbf{q}) = \left(\frac{\partial h}{\partial T} \right)_{P,y} = \sum_{i=1}^{NS} y_i(T, P, \mathbf{q}) c_{p_{ii}}(T, P), \quad (31)$$

$$c_{v,\text{off}}(T, P, \mathbf{q}) = \left(\frac{\partial u}{\partial T} \right)_{v,y} = \sum_{i=1}^{NS} y_i(T, P, \mathbf{q}) c_{v_{ii}}(T, P) = c_{p,\text{off}}(T, P, \mathbf{q}) - \frac{\bar{R}}{M_t(T, P, \mathbf{q})}, \quad (32)$$

$$\gamma_{\text{off}}(T, P, \mathbf{q}) = \frac{c_{p,\text{off}}(T, P, \mathbf{q})}{c_{v,\text{off}}(T, P, \mathbf{q})} = \left(1 - \frac{\bar{R}}{M_t(T, P, \mathbf{q}) c_{p,\text{off}}(T, P, \mathbf{q})} \right)^{-1}, \quad (33)$$

$$\gamma_{s,\text{off}}(T, P, \mathbf{q}) = \frac{\rho}{P} \left(\frac{\partial P}{\partial \rho} \right)_{s,y} = \gamma_{\text{off}} \frac{\rho}{P} \left(\frac{\partial P}{\partial \rho} \right)_{T,y} = \gamma_{\text{off}}(T, P, \mathbf{q}), \quad (34)$$

$$\chi_{\text{off}}(T, P, \mathbf{q}) = \sqrt{\left(\frac{\partial P}{\partial \rho} \right)_{s,y}} = \sqrt{\frac{\gamma_{\text{off}}(T, P, \mathbf{q}) \bar{R}T}{M_t(T, P, \mathbf{q})}}, \quad (35)$$

with y the mass fraction, and where of course, we used the Meyer relations, $c_{p_{ii}} = c_{v_{ii}} + \bar{R}/M_i$. Equilibrium specific heats at constant pressure will be calculated as:

$$c_{p,\text{eq}} = \left(\frac{\partial h}{\partial T} \right)_{P,\mathbf{q}} = \sum_{i=1}^{NS} y_i c_{p_{ii}}(T, P) + \sum_{i=1}^{NS} h_{ii}(T, P) \left(\frac{\partial y_i}{\partial T} \right)_{P,\mathbf{q}}. \quad (36)$$

All of the above properties can be easily computed if the following three properties are known as functions of temperature T and pressure P , for the given elemental

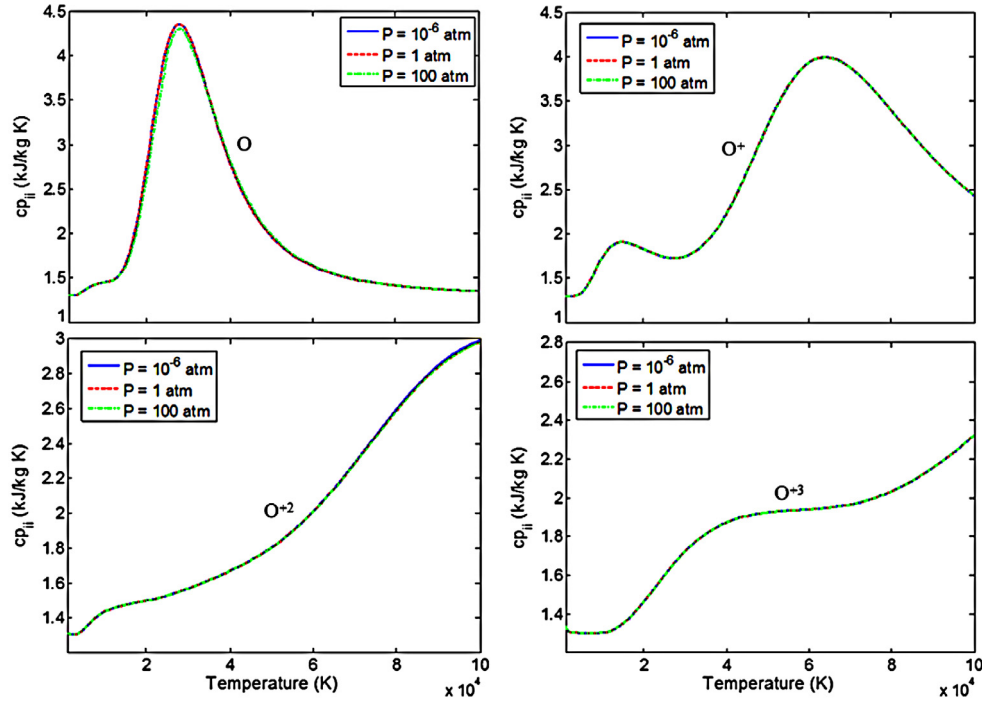


Fig. 3. Specific heat at constant pressure for oxygen atom and its ions versus temperature for three different pressures, 10^{-6} , 1 and 100 atm.

composition \mathbf{q}

$$g = g(T, P, \mathbf{q}) \quad (37)$$

$$M_t = M_t(T, P, \mathbf{q}) \quad (38)$$

$$c_{p,\text{off}} = c_{p,\text{off}}(T, P, \mathbf{q}). \quad (39)$$

Indeed, for example, from the latter we can find

$$s = -\frac{\partial g(T, P, \mathbf{q})}{\partial T},$$

$$\frac{c_{p,\text{eq}}}{T} = \left(\frac{\partial s}{\partial T}\right)_{P, \mathbf{q}} = -\frac{\partial^2 g(T, P, \mathbf{q})}{\partial T^2},$$

$$\left(\frac{\partial s}{\partial P}\right)_{T, \mathbf{q}} = -\frac{\partial^2 g(T, P, \mathbf{q})}{\partial T \partial P} \quad (40)$$

and similarly from $h = g + Ts$ and $u = h - \overline{RT}/M_t$ we may find all the other partial derivatives. It is for this reason that in Section 3.5 we propose correlations for the relations (37), (38) and (39) (see Eqs. (47), (48) and (43) respectively). The coefficients for these correlations have been obtained by running the complete chemical equilibrium composition calculations for various temperatures, pressures, and initial compositions, so as to compute the mass fractions $y_i(T, P, \mathbf{q})$ needed in the relations (26), (27) and (31), which lead to relations (37), (38) and (39). In Section 3.5 we discuss the functional forms chosen to correlate efficiently these relations. The coefficients for hydrogen-air and methane-air plasmas are listed in Appendix.

3.4 Ideal gas model validation

As part of the preliminary computations, we checked the validity of the ideal gas model assumption. In order to consider an ionized gas as an ideal one, it is necessary that the energy of the Coulomb interaction between neighboring particles be small in comparison with the thermal energy of the particles [53], meaning

$$N_t \ll \left(\frac{kT}{\Lambda^2 e^2}\right)^3 = 2.2 \times 10^{14} \left(\frac{T}{\Lambda^2}\right)^3 \quad [\text{m}^{-3}], \quad (41)$$

where N_t is the number density of the plasma mixture, Λ is the degree of ionization defined as

$$\Lambda = \frac{N_I}{N_I + N_n}, \quad (42)$$

where N_I is the number density of ions and N_n is the number density of neutral atoms. The virial corrections to thermodynamic properties are negligible especially for temperatures higher than 2000 K and pressures up to 1000 atm [54,55]. Virial corrections have very significant effects for very low temperatures and very high pressures [56] meaning far from plasma conditions. Inequality (41) is comfortably satisfied for all plasmas at all pressure and temperatures considered in this work.

3.5 Fitting of thermodynamic properties

It is desired to have analytical expressions to evaluate the thermodynamic properties of a plasma mixture without

iteration. Such expression would be valuable for example as a subroutine in a computer program or a CFD code. Fitting thermodynamic functions for plasma mixture properties in a wide range of temperatures (1000–100 000 K) and pressures (10^{-6} – 10^2 atm) is a complicated problem because of the non-monotonic behavior of some properties as functions of temperature, in particular, the equilibrium specific heat $c_{p,eq}$. In order to correlate the computed values of $c_{p,eq}$, we have chosen a modified Hill equation in conjunction with a modified Log-normal distribution function. These functions provide the capability to capture the peaks and valleys of the equilibrium specific heat. The number of terms for first (modified Hill) part of the $c_{p,eq}$ correlation depends on how well we can fit $c_{p,off}$ to the exact data points and the number of terms for the second (modified Log-normal) part depends on the number of peaks in $c_{p,eq}$.

The least squares fitting procedure is as follows. First we find the coefficients for $c_{p,eq}$, then we find the coefficients for the integration constants of the specific enthalpy and the specific entropy obtained by integration of the functional form of the correlation for $c_{p,eq}$ according to $h = \int c_{p,eq} dT + \text{const}$ and $s = \int (c_{p,eq}/T) dT + \text{const}$ respectively. The integration constants are obtained by least square fitting the calculated data for enthalpy and entropy to the correlations developed by integration. The advantage of this approach is that the main set of coefficients for the equilibrium specific heat, the specific enthalpy and the specific entropy are the same and are consistent with the thermodynamic relations provided in the previous sections.

Below, we present the analytical expressions that we propose for the correlations of the frozen and equilibrium specific heat at constant pressure, the specific enthalpy, the specific entropy, the specific Gibbs free energy, and the mean molar mass. The results of the least square fittings of our calculated data using these correlations are given in Appendix. The number of terms in the summations have been chosen so that the relative errors of the correlations are always less than 2%.

Frozen specific heat at constant pressure (kJ/kg K)

$$c_{p,off} = \sum_{i=1}^8 \frac{a_i^{off}}{1 + (b_i^{off}/T)^{c_i^{off}}}. \quad (43)$$

Equilibrium specific heat at constant pressure (kJ/kg K)

$$c_{p,eq} = \sum_{i=1}^8 \frac{a_i^{off}}{1 + (b_i^{off}/T)^{c_i^{off}}} + \sum_{i=9}^{16} a_i^{eq} \exp \left[- \left(\frac{\ln(T/b_i^{eq})}{c_i^{eq}} \right)^2 \right]. \quad (44)$$

Specific enthalpy (kJ/kg)

$$h = \lambda_1 + T \sum_{i=1}^8 a_i^{off} \left(1 - {}_2F_1 \left(1, \frac{1}{c_i^{off}}, 1 + \frac{1}{c_i^{off}}, - \left(\frac{T}{b_i^{off}} \right)^{c_i^{off}} \right) \right) - \frac{\sqrt{\pi}}{2} \sum_{i=9}^{16} a_i^{eq} b_i^{eq} c_i^{eq} \exp \left(\frac{(c_i^{eq})^2}{4} \right) \times \text{erf} \left(\frac{c_i^{eq}}{2} - \frac{\ln(T/b_i^{eq})}{c_i^{eq}} \right). \quad (45)$$

Specific entropy (kJ/kg K)

$$s = \lambda_2 + \sum_{i=1}^8 \frac{a_i^{off}}{c_i^{off}} \ln \left((b_i^{off})^{c_i^{off}} + (T)^{c_i^{off}} \right) + \frac{\sqrt{\pi}}{2} \sum_{i=9}^{16} a_i^{eq} c_i^{eq} \text{erf} \left(\frac{\ln(T/b_i^{eq})}{c_i^{eq}} \right), \quad (46)$$

where erf and ${}_2F_1(a, b, c, x)$ are the error function and the hypergeometric functions², respectively. As a result of equations (45) and (46), the specific Gibbs free energy is

$$g = \lambda_1 - T\lambda_2 + T \sum_{i=1}^8 a_i^{off} \left(1 - {}_2F_1 \left(1, \frac{1}{c_i^{off}}, 1 + \frac{1}{c_i^{off}}, - \left(\frac{T}{b_i^{off}} \right)^{c_i^{off}} \right) \right) - T \sum_{i=1}^8 \frac{a_i^{off}}{c_i^{off}} \ln \left((b_i^{off})^{c_i^{off}} + (T)^{c_i^{off}} \right) - \frac{\sqrt{\pi}}{2} \sum_{i=9}^{16} a_i^{eq} b_i^{eq} c_i^{eq} \exp \left(\frac{(c_i^{eq})^2}{4} \right) \times \text{erf} \left(\frac{c_i^{eq}}{2} - \frac{\ln(T/b_i^{eq})}{c_i^{eq}} \right) - \frac{T\sqrt{\pi}}{2} \sum_{i=9}^{16} a_i^{eq} c_i^{eq} \text{erf} \left(\frac{\ln(T/b_i^{eq})}{c_i^{eq}} \right). \quad (47)$$

Mean molar mass (kg/kmol)

$$M_t = \lambda_3 - \sum_{i=1}^8 \frac{a_i^M}{1 + (b_i^M/T)^{c_i^M}}, \quad (48)$$

where the various coefficients are function of pressure and equivalence ratio using polynomial surface (PS_{mn})

² <http://www.mathworks.com/matlabcentral/fileexchange/43865-gauss-hypergeometric-function/content/hyp2f1mex/hyp2f1.m>, p. 43865.

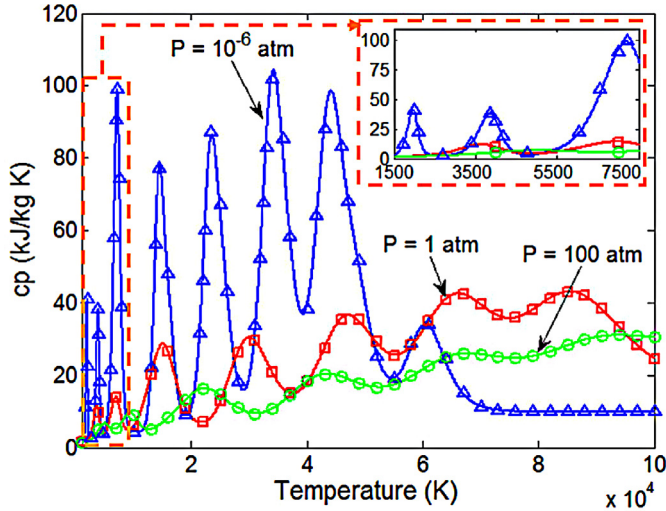


Fig. 4. Comparison between calculated data (solid line) and fitted data (symbols) for the equilibrium specific heat at constant pressure $c_{p,eq}$ of a stoichiometric H_2 /air plasma mixture for $P = 10^{-6}$, 1 and 10^2 atm.

of degree m in ϕ and degree n in $\ln(P)$ as follows,

$$PS_{mn} = \xi_{00} + \sum_{i=1}^m \xi_{i0} \phi^i + \sum_{j=1}^n \xi_{0j} (\ln(P))^j + \begin{cases} \sum_{k=1}^m \sum_{l=1}^{n-k} \xi_{kl} \phi^k (\ln(P))^l & \text{for } m < n \\ \sum_{k=1}^{n-1} \sum_{l=1}^{n-l} \xi_{kl} \phi^k (\ln(P))^l & \text{for } m = n \\ \sum_{l=1}^n \sum_{k=1}^{m-l} \xi_{kl} \phi^k (\ln(P))^l & \text{for } m > n \end{cases} \quad (49)$$

$$a, b, c = \exp(PS_{mn}) \quad (50)$$

$$\lambda = PS_{mn}. \quad (51)$$

The degree of m and n for methane/air mixture are considered 2 and 5, respectively. For hydrogen/air mixture we have two sets of degree, first one is $m = 4$ and $n = 3$ and the second one is $m = 5$ and $n = 2$ to provide the best fit. In this way all the thermodynamic properties are expressed as a function temperature, pressure and equivalence ratio. The values of the ξ_{kl} coefficients that result from our least square fitting procedure are reported in Appendix for H_2 /air and CH_4 /air plasma mixtures in Tables A.2 and A.3, respectively. Figure 4 shows the comparison of the equilibrium specific heat at constant pressure for H_2 /air plasma mixtures between calculated and fitted data which indicates excellent agreement.

4 Results and discussion

In this section we present and discuss some of our calculated chemical equilibrium compositions and thermodynamic properties for H_2 /air and CH_4 /air plasmas in the temperature range 1000–100000 K, pressure range

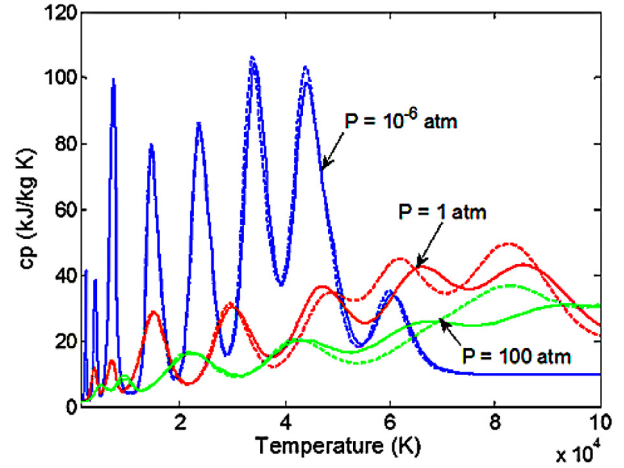


Fig. 5. Comparison of values of the equilibrium specific heat at constant pressure $c_{p,eq}$ computed using our self-consistent method (solid line) and the so-called ground state method (dashed line), for a stoichiometric H_2 /air plasma at three different pressures, 10^{-6} , 1 and 100 atm.

10^{-6} – 10^2 atm, and for different equivalence ratios within flammability limits (for methane/air mixture flammability limit is $0.6 < \phi < 1.4$ and for hydrogen/air mixture flammability limit is $0.5 < \phi < 5.0$). Calculated values have been fitted using the analytical correlations proposed in the previous section and the fitting coefficients are tabulated in Appendix.

Figure 5 shows an important effect that must be carefully taken into account in the interest of accuracy, namely, the effect of the excited energy levels on the specific heat at constant pressure for stoichiometric H_2 /air plasma mixture. Figure 5 compares the results obtained using our self-consistent method considering excited energy levels with those of the so-called *ground state* method. As it can be seen, for temperatures below 15000 K the effect of excited energy levels on the values of the specific heat and hence all the properties is negligible, because at relatively low temperatures the high order terms in the electronic partition function expansion are indeed negligible. But for temperatures above 15000 the effect is significant and, importantly, it exhibits a strong pressure dependence. The reason is that, differently from the ground state method, our self-consistent method takes into account the experimental observation that the number of excited energy levels is a function of both temperature and pressure. In other words, Figure 5 shows that considering just the ground state or fixing the number of excited energy levels independent of pressure, may introduce very large errors in the estimated thermodynamic properties at high plasma temperatures, especially for derivative properties like the specific heats.

In order to validate our calculations with data existing in the literature for high temperature plasmas, due to lack of data for H_2 /air and CH_4 /air plasma mixtures at high temperatures, we make a comparison with air plasma. The reasons to choose air are that first it forms a large portion of typical fuel/air mixtures and also many researches

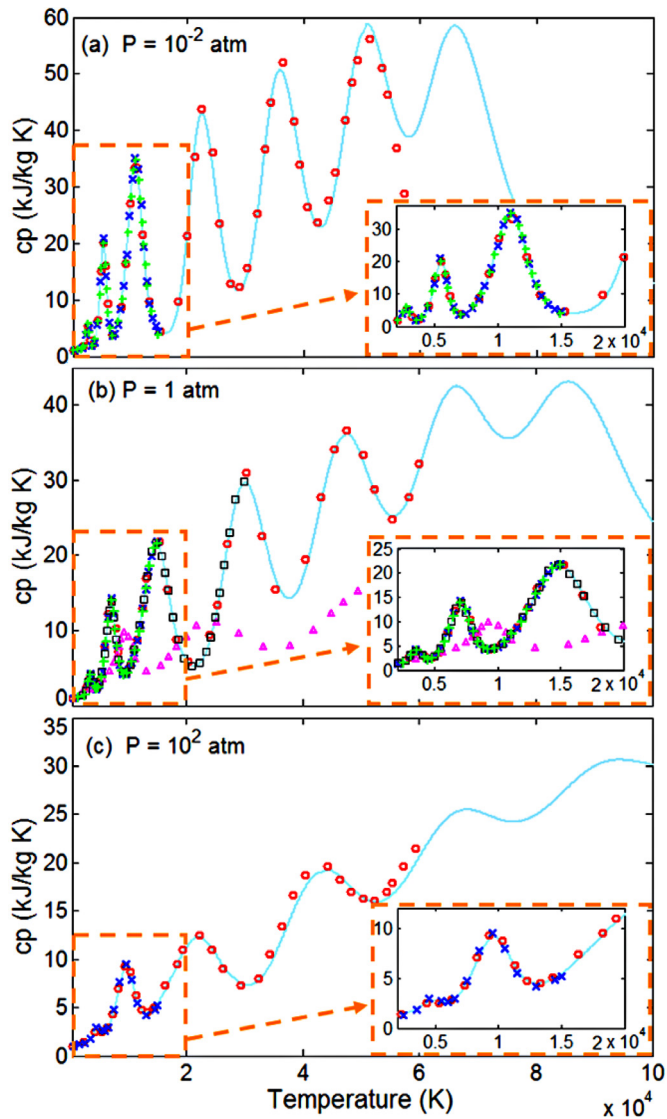


Fig. 6. Comparisons of the values of the equilibrium specific heats at constant pressure $c_{p,eq}$ of air plasma mixture obtained with present study (solid line) and those obtained by D’Angola et al. [25] (o), Hansen [6] (x), Sher et al. [19] (Δ), Cressault et al. [57] (\square) and Bottin [58] (+) for three different pressures: (a) = 10^{-2} , (b) = 1, and (c) = 100 atm.

have already been done on air plasma. Figure 6 compares the equilibrium specific heat at constant pressure of air plasma calculated in this study with those of D’Angola et al. [25] (up to 60 000 K), Hansen [6] (up to 15 000 K), Sher et al. [19] (up to 50 000 K), Cressault et al. [57] (up to 30 000 K), and Bottin [58] (up to 15 000 K) for three different pressures, 10^{-2} , 1, and 100 atm. The data for Sher et al. [19] and Cressault et al. [57] are available only for atmospheric pressure. The underestimate in Sher et al.’s results is due to the very simple method he used to find individual properties. The results of this study are shown an excellent agreement in low and high pressures with D’Angola et al. [25] (up to 60 000 K). Figure 7 compares the equilibrium compositions of air plasma com-

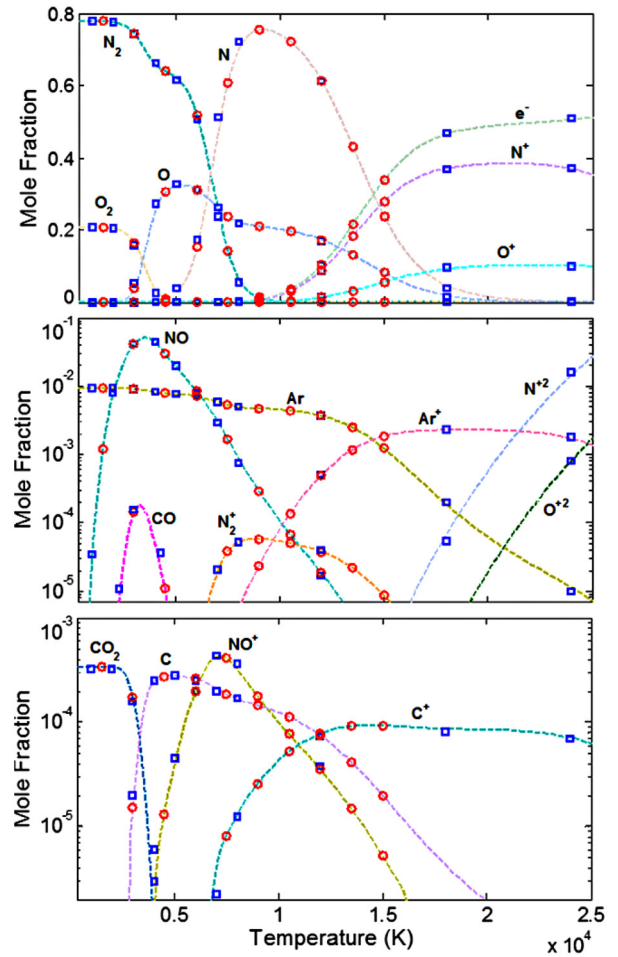


Fig. 7. Comparisons of the selected species mole fraction of air plasma mixture obtained with present study (dashed line) and those obtained by Gilmore [2] (\square) and Hilsenrath and Klein [54] (o) at pressure of 1 atm.

puted in this study with tabulated data by Hilsenrath and Klein [54] (up to 15 000 K) and Gilmore [2] (up to 24 000 K) at atmospheric pressure for temperature range of 300 to 25 000 K. As it is obvious from Figures 6 and 7, the results of our calculations are in very good agreement with existing data, in spite of the slight differences in air composition assumed in the different studies. We are now in the position to examine our results to illustrate the important effects of temperature and pressure on all properties. Figure 8 shows the mole fractions of the neutral and ionized single species (only those with mole fractions greater than 2×10^{-6}) for a stoichiometric CH_4/air plasma mixture at atmospheric pressure.

Figure 9 shows the mean molar mass M_t and the degree of ionization Λ , over the temperature range 1000–100 000 K for different pressures (10^{-6} , 1, and 100 atm) for a stoichiometric H_2/air plasma. As shown in Figure 9a, increasing the temperature at a given pressure leads to a decrease in mean molar mass due to the increase in mole numbers resulting from dissociation. The stepwise decrease in the molar mass is connected to the successive

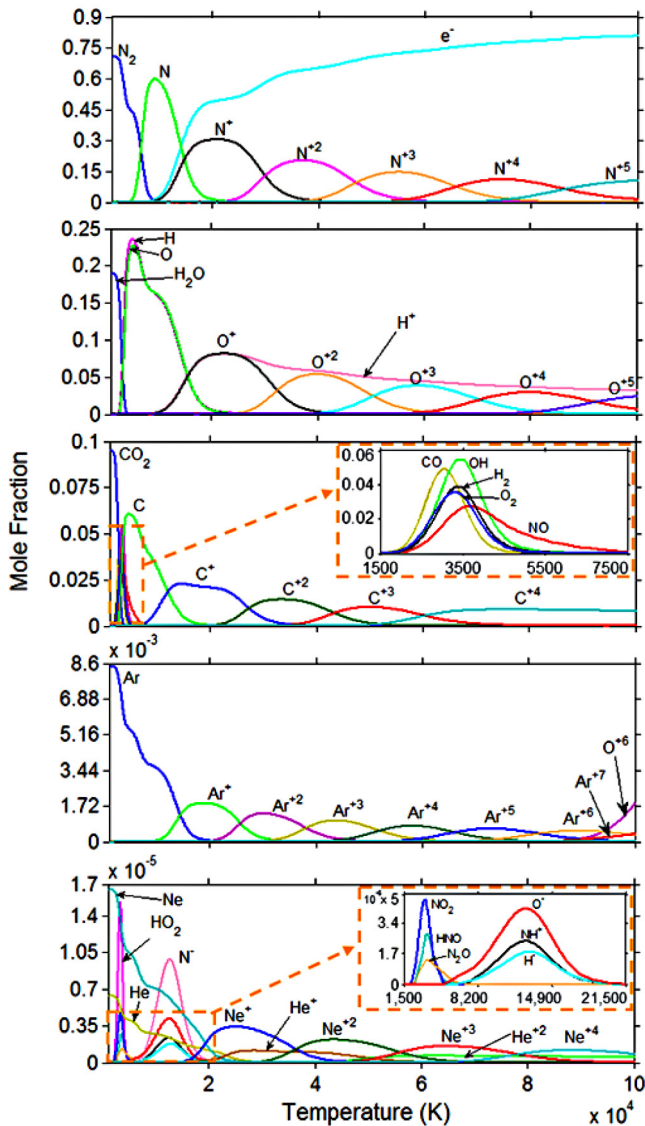


Fig. 8. Mole fractions for selected species in a stoichiometric CH_4/air plasma at atmospheric pressure.

ionization of atomic species, while the slope becomes zero in transitions from one ionization to another. This behavior is very manifest at low pressures and becomes less evident at high pressures. The dissociation reactions are significantly favored at low pressures and consequently the transition from partially ionized gas ($\Lambda < 1$) to fully ionized gas ($\Lambda = 1$) takes place at lower temperature for low pressures than for high pressure. This is seen in Figure 9b, where the fully ionized condition for $P = 10^{-6}$ atm obtains around 10 000 K whereas for $P = 100$ atm it occurs around 50 000 K.

Figure 10a shows the equilibrium specific heat at constant pressure for a stoichiometric CH_4/air plasma mixture. It shows some distinct peaks with increasing temperature where the temperature dependence of the complete chemical equilibrium composition is very high. These peaks are connected first to dissociation of the molecules

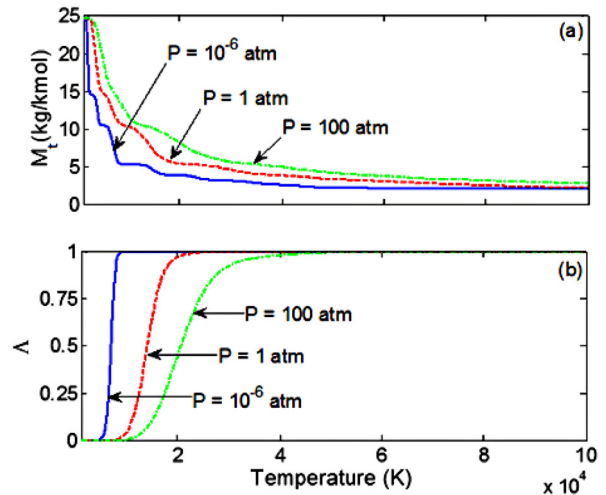


Fig. 9. (a) Mean molar mass M_t and (b) degree of ionization Λ at three different pressures (10^{-6} , 1 and 100 atm) for a stoichiometric H_2/air plasma mixture.

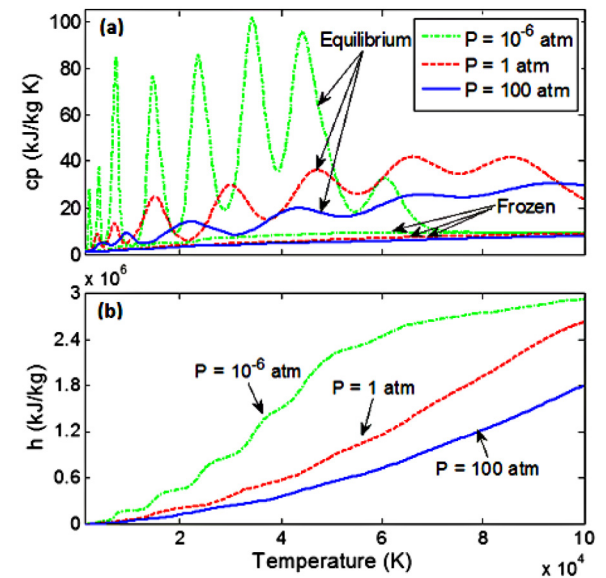


Fig. 10. (a) Equilibrium and frozen specific heat at constant pressure $c_{p,eq}$ and (b) specific enthalpy for a stoichiometric CH_4/air plasma mixture at three different pressures, 10^{-6} , 1 and 100 atm.

and then to successive ionization of the atomic species. When pressure decreases the peaks become sharper and shift to lower temperature. This effect, again, is due to the favorable effect of low pressure on dissociation and ionization reactions. As a result, for each given temperature, more chemical energy is stored at low pressure, resulting in the specific enthalpy of the plasma mixture being a decreasing function of pressure, as shown in Figure 10b. Figure 10a compares the frozen and equilibrium specific heats at constant pressure, $c_{p,off}$ and $c_{p,eq}$, defined by equations (31) and (36), respectively, for a stoichiometric CH_4/air plasma at different pressures. As it can be

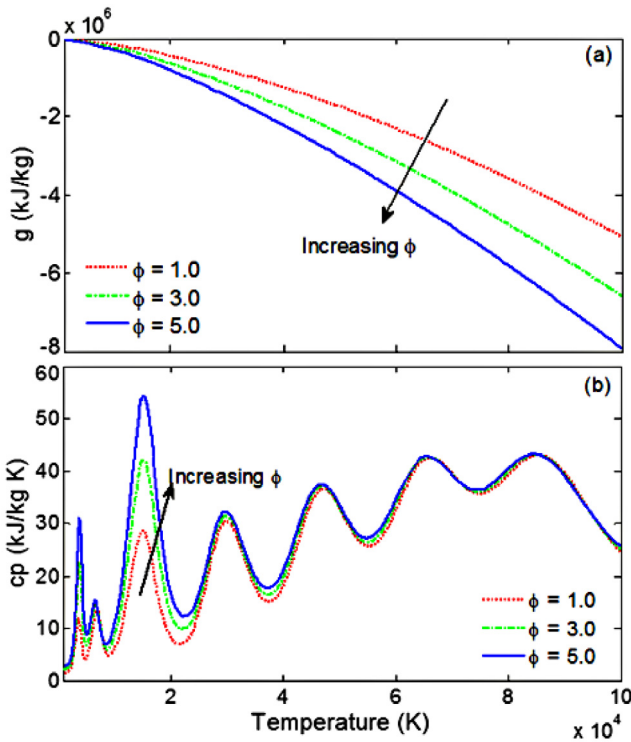


Fig. 11. (a) Gibbs free energy and (b) equilibrium specific heat at constant pressure for a H_2 /air plasma mixture at atmospheric pressure for three different equivalence ratio of 1, 3 and 5.

seen, the effect of chemistry is clearly visible and whenever dissociation and ionization start to play a role and become important, $c_{p,eq}$ presents a peak. When maximum ionization is reached in the mixture, no further reactions take place, so the rates of change of mole fractions with temperature, $(\partial y_i / \partial T)_{P,q}$, become small and values of equilibrium $c_{p,eq}$ decrease and reach the frozen $c_{p,off}$ values. This behavior is shown in Figure 10a for the pressure of 10^{-6} atm around 75 000 K. It is important to emphasize again that the pressure dependence of the mixture enthalpy and equilibrium specific heat has two significant reasons. One is the pressure dependence of the complete chemical equilibrium composition and its rate of change with temperature. In fact, chemical composition, computed with the complete equilibrium method which is a function of pressure. The second reason is related to the electronic partition functions of the individual species, which depend on the cut-off criteria that determine the maximum number of energy levels that need to be considered. As discussed in Section 2.2.2.1, our cut-off criteria are functions of the Debye length, which in turn is related to number densities and, hence, to pressure.

Figure 11 shows the effect of equivalence ratio on the specific Gibbs free energy and the equilibrium specific heat at constant pressure for H_2 /air plasma mixture. At each given temperature, the Gibbs free energy is a decreasing function of equivalence ratio whereas the equilibrium specific heat at constant pressure increases with equivalence ratio. The effect on the specific heat is most significant at

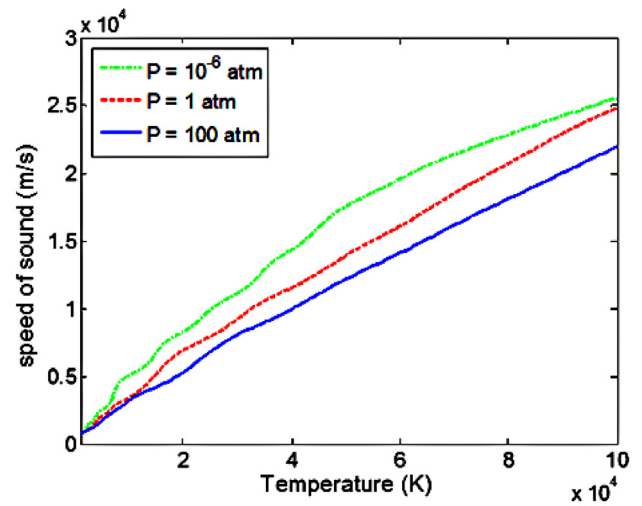


Fig. 12. Speed of sound in a stoichiometric H_2 /air plasma mixture at three different pressures, 10^{-6} , 1 and 100 atm.

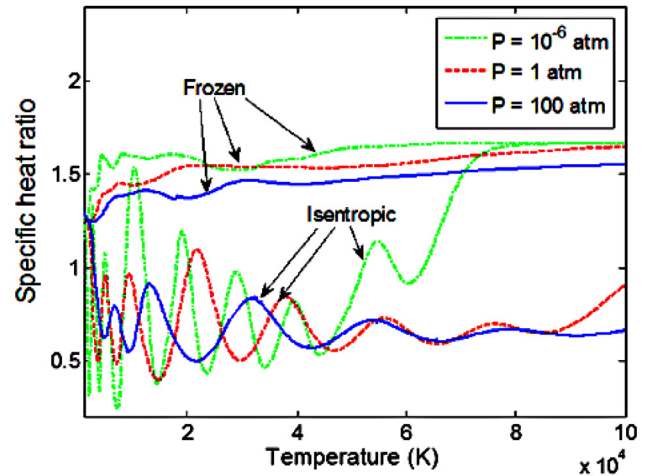


Fig. 13. Specific heat ratio γ_{off} and isentropic exponent $\gamma_{s,off}$ for a stoichiometric CH_4 /air plasma mixture at three different pressures of 10^{-6} , 1 and 100 atm.

the first and third peaks, around 3800 K and 15 000 K, respectively. As already seen in Figure 8, the 3800 K peak is due to the dissociation reaction to create atomic hydrogen, while the 15 000 K peak is due to the ionization reaction to form ionic hydrogen. Increasing the equivalence ratio is equivalent to increasing the hydrogen percentage in the mixture and therefore the more hydrogen in the mixture the more hydrogen dissociation and ionization reactions contribute to the mixture properties.

Figure 12 shows speed of sound χ_{off} defined by equation (35). Speed of sound is higher at low pressures, leading to higher Mach numbers for each given temperature. The differences between frozen specific heat ratio γ_{off} defined by equation (33) and isentropic exponent $\gamma_{s,off}$ defined by equation (34) are shown in terms of pressure and temperature in Figure 13. As it can be seen in Figure 13, the frozen specific heat ratio is higher at low pressures and the isentropic exponent is always lower

than its corresponding specific heat ratio. Under the condition of non-reacting flows or when maximum ionization is reached in the mixture, the rates of change of mass fractions with respect to temperature become negligible and the ratio of specific heats and the isentropic exponent become identical as it is shown in Figure 13 for the pressure of 10^{-6} atm. For higher pressures this convergence happens in higher temperatures.

5 Conclusion

A comprehensive model has been developed to calculate thermodynamic properties of hydrogen/air and methane/air plasma up to 100 000 K for a wide range of pressures and fuel/air equivalence ratios. The model is based on statistical thermodynamics and complete chemical equilibrium of all species. For both hydrogen/air and methane/air plasma mixtures the model considers 133 species. Properties such as enthalpy, entropy, Gibbs free energy, specific heat at constant pressure, specific heat ratio, speed of sound, mean molar mass, and degree of ionization have been calculated. The results have been compared to available experimental data and the agreement is excellent. For each mixture and fuel/air equivalence ratio considered, the properties have been summarized in the form of curve-fitted correlations as suitably defined functions of temperature, pressure and equivalence ratio. In addition, the results have also allowed the following conclusions relevant for other existing state-of-the-art models of thermodynamic properties:

1. considering just the ground state or fixing the number of energy levels independently of the temperature and the pressure produces very large errors in the estimates

especially for second order properties at high temperature conditions. In particular, the accuracy of the ground state method accuracy decreases with increasing the pressure and temperature;

2. transition from partially ionized gas ($\Lambda < 1$) to fully ionized gas ($\Lambda = 1$) takes place at relatively low temperatures;
3. the speed of sound is higher at low pressures, leading to higher Mach numbers at low pressures for each given temperature.

This paper was made possible by NPRP award [NPRP 7-1449-2-523] from Qatar National Research Fund (a member of the Qatar Foundation). This statement is solely the responsibility of the authors.

Appendix: Fitting coefficients for hydrogen/air and methane/air plasma mixtures

In this supplementary material we present the coefficients to calculate frozen and equilibrium specific heat at constant pressure, specific enthalpy, specific entropy, and mean molar mass, according to equations (43), (44), (45), (46) and (48), respectively, for hydrogen-air and methane-air plasma mixtures. For our calculations and correlations, we assumed the following molar composition of air (no water vapor): $x_{\text{N}_2}^{\text{a}} = 0.78084$, $x_{\text{O}_2}^{\text{a}} = 0.20946$, $x_{\text{H}_2\text{O}}^{\text{a}} = 0$, $x_{\text{Ar}}^{\text{a}} = 0.009335$, $x_{\text{CO}_2}^{\text{a}} = 0.0003398$, $x_{\text{Ne}}^{\text{a}} = 0.00001818$, $x_{\text{He}}^{\text{a}} = 0.00000702$. Table A.1 gives the corresponding values of the q_j 's that we considered, as functions of the equivalence ratio ϕ . Tables A.2 and A.3 show the fitting coefficients of hydrogen/air and methane/air plasma mixture, respectively.

Table A.1. Values of the q_j 's as a function of the equivalence ratio ϕ .

Elemental atom numbers	C_kH_l /air mixture	H_2 /air mixture ($k = 0, l = 2$)	CH_4 /air mixture ($k = 1, l = 4$)
q_{N}	$\frac{1}{\phi} \left(k + \frac{l}{4} \right) \frac{2x_{\text{N}_2}^{\text{a}}}{x_{\text{O}_2}^{\text{a}}}$	$\frac{0.78084}{0.20946\phi}$	$\frac{4 \times 0.78084}{0.20946\phi}$
q_{O}	$\frac{1}{\phi} \left(k + \frac{l}{4} \right) \left(2 + \frac{x_{\text{H}_2\text{O}}^{\text{a}}}{x_{\text{O}_2}^{\text{a}}} + \frac{2x_{\text{CO}_2}^{\text{a}}}{x_{\text{O}_2}^{\text{a}}} \right)$	$\frac{1}{\phi} + \frac{0.0003398}{0.20946\phi}$	$\frac{4}{\phi} + \frac{4 \times 0.0003398}{0.20946\phi}$
q_{C}	$k + \frac{1}{\phi} \left(k + \frac{l}{4} \right) \frac{x_{\text{CO}_2}^{\text{a}}}{x_{\text{O}_2}^{\text{a}}}$	$\frac{0.5 \times 0.0003398}{0.20946\phi}$	$1 + \frac{2 \times 0.0003398}{0.20946\phi}$
q_{H}	$l + \frac{1}{\phi} \left(k + \frac{l}{4} \right) \frac{2x_{\text{H}_2\text{O}}^{\text{a}}}{x_{\text{O}_2}^{\text{a}}}$	2	4
q_{Ar}	$\frac{1}{\phi} \left(k + \frac{l}{4} \right) \frac{x_{\text{Ar}}^{\text{a}}}{x_{\text{O}_2}^{\text{a}}}$	$\frac{0.5 \times 0.009335}{0.20946\phi}$	$\frac{2 \times 0.009335}{0.20946\phi}$
q_{Ne}	$\frac{1}{\phi} \left(k + \frac{l}{4} \right) \frac{x_{\text{Ne}}^{\text{a}}}{x_{\text{O}_2}^{\text{a}}}$	$\frac{0.5 \times 0.00001818}{0.20946\phi}$	$\frac{2 \times 0.00001818}{0.20946\phi}$
q_{He}	$\frac{1}{\phi} \left(k + \frac{l}{4} \right) \frac{x_{\text{He}}^{\text{a}}}{x_{\text{O}_2}^{\text{a}}}$	$\frac{0.5 \times 0.00000702}{0.20946\phi}$	$\frac{2 \times 0.00000702}{0.20946\phi}$

Table A.2. H₂/air plasma.

	ξ_{00}	ξ_{10}	ξ_{01}	ξ_{20}	ξ_{11}	ξ_{02}	ξ_{30}	ξ_{21}	ξ_{12}	ξ_{03}	ξ_{40}	ξ_{31}	ξ_{22}	ξ_{13}
a_1^{off}	0.325766	0.295999	-0.010454	0.17606	0.016251	0.000125	-7.51E-02	-0.004551	-0.000141	2.02E-06	0.007738	3.92E-04	1.55E-06	6.11E-07
a_2^{off}	-0.356532	0.20411	-0.014564	-0.321786	0.053117	-0.009868	0.087119	-0.021719	0.004184	-0.00035	-0.006685	2.42E-03	-1.63E-04	1.05E-04
a_3^{off}	0.149062	0.482639	0.01784	-0.141731	-0.005376	0.004729	0.031576	0.002638	-0.001093	0.000193	-2.84E-03	-2.99E-04	3.68E-05	-4.42E-05
a_4^{off}	0.492105	-0.027053	0.009439	-0.07043	-0.016436	3.66E-04	0.02252	0.001266	-0.001508	4.44E-05	-2.13E-03	-6.75E-05	3.66E-05	-5.54E-05
a_5^{off}	0.495306	0.046521	-0.027897	-0.065072	0.005746	-1.37E-04	0.017576	-0.000864	9.96E-04	2.38E-05	-0.001632	-4.31E-05	-7.25E-05	3.74E-05
a_6^{off}	-0.246024	0.260661	-0.111618	-0.240513	0.032134	-0.019551	0.072196	0.000282	5.70E-03	-0.000876	-6.88E-03	-2.39E-04	-1.77E-04	2.08E-04
a_7^{off}	-0.052569	0.500379	0.008356	-0.295294	0.039514	-0.000679	0.058712	-0.015687	0.000776	-6.94E-05	-4.01E-03	1.57E-03	-0.000109	2.49E-05
a_8^{off}	-1.316139	-0.63594	0.002881	0.208148	-0.047142	-0.005715	-0.021114	0.0235	0.003315	-0.000247	-0.000488	-2.87E-03	-4.53E-05	1.69E-04
b_1^{off}	5.723293	1.02107	-0.002698	-0.511197	0.005373	-4.85E-05	0.109718	-0.00247	0.000164	6.60E-06	-0.008195	3.12E-04	-5.76E-05	-4.07E-06
b_2^{off}	8.952488	-0.065389	0.038513	0.044519	0.007632	-0.001154	-0.013942	-0.005278	0.002049	-7.46E-05	1.74E-03	7.08E-04	-1.66E-04	7.60E-05
b_3^{off}	9.591297	0.005342	0.060889	-0.004212	-0.000505	-8.48E-05	0.00092	-0.000135	1.79E-05	-5.08E-05	-5.58E-05	2.63E-05	4.00E-06	4.05E-06
b_4^{off}	10.31002	-0.003176	0.061256	0.00335	0.000614	0.000559	-0.000694	1.23E-04	6.00E-05	-1.52E-05	5.39E-05	-7.52E-06	2.53E-06	1.05E-06
b_5^{off}	10.75484	-0.004941	0.066266	-0.00014	-0.000329	0.001644	0.000297	1.07E-04	3.33E-05	2.87E-05	-3.99E-05	-1.43E-05	-1.69E-06	1.81E-06
b_6^{off}	11.09656	0.005438	0.054597	-0.00577	0.002364	0.000248	0.001791	-0.00011	3.96E-04	-2.90E-05	-1.80E-04	-1.59E-05	-1.85E-05	1.46E-05
b_7^{off}	11.33268	0.059837	0.043133	-0.035995	0.00807	-0.001844	0.008301	-0.001454	8.33E-04	-0.000124	-6.66E-04	1.10E-04	-3.54E-05	3.12E-05
b_8^{off}	11.03422	1.089476	-0.009898	-0.513685	0.109938	0.001625	0.083932	-0.041693	1.03E-03	0.000145	-0.004116	4.20E-03	-3.60E-04	-3.94E-05
c_1^{off}	0.124054	0.840514	0.040843	-1.210174	-0.072285	-5.72E-05	0.385634	0.019032	0.000658	5.78E-06	-3.67E-02	-1.57E-03	-3.99E-05	1.01E-06
c_2^{off}	2.271393	-0.172845	-0.019733	0.074026	0.032179	-0.003477	-0.021718	-0.009678	0.00277	-0.00016	0.001756	4.71E-04	-1.35E-04	8.93E-05
c_3^{off}	2.48469	-0.032591	-0.045116	0.046243	-0.00277	-0.006517	-0.01555	-0.000701	0.000415	-0.000372	1.63E-03	1.44E-04	-1.90E-05	2.07E-05
c_4^{off}	2.601802	0.023603	-0.043885	0.047296	0.010316	-0.003402	-0.016312	-0.001063	7.96E-04	-1.53E-04	1.57E-03	8.14E-05	-9.97E-06	3.36E-05
c_5^{off}	2.593675	-0.043896	-0.053577	0.029797	-0.008094	-0.000805	-0.006784	0.001325	-0.001015	5.52E-05	0.000612	1.13E-05	7.98E-05	-3.51E-05
c_6^{off}	2.82907	0.023139	-0.028702	0.007746	-0.004316	0.003463	-0.007304	-0.002063	-1.31E-03	0.000248	0.000934	2.58E-04	3.88E-05	-3.72E-05
c_7^{off}	2.617703	0.025931	-0.032416	-0.096552	-0.031419	-0.001768	0.042323	0.012062	-0.000329	-5.35E-05	-4.70E-03	-9.89E-04	0.000225	3.05E-05
c_8^{off}	2.679309	0.188426	-0.078739	-0.038423	0.023823	-0.003399	-0.007311	-0.009759	0.001192	-8.77E-05	0.001749	0.001131	-5.83E-06	8.23E-05

Table A.2. Continued.

	ξ_{00}	ξ_{10}	ξ_{01}	ξ_{20}	ξ_{11}	ξ_{02}	ξ_{30}	ξ_{21}	ξ_{12}	ξ_{40}	ξ_{31}	ξ_{22}	ξ_{13}
	$c_{p,off}$ (kJ/kg K), $c_{p,eq}$ (kJ/kg K), h (kJ/kg), s (kJ/kg K)												
a_1^{eq}	1.258564	1.515934	-0.133356	-0.585117	-0.005996	-0.00369	1.15E-01	0.001849	4.65E-05	-5.48E-05	-8.53E-03	-1.75E-04	-2.57E-05
a_2^{eq}	2.495274	-0.006412	-0.101442	-0.001124	0.003565	-0.001871	-0.00025	-0.000344	0.000359	-2.60E-05	7.38E-05	5.31E-05	9.25E-07
a_3^{eq}	2.92697	0.351267	-0.135045	-0.065859	0.001769	-0.004247	0.009786	-0.001006	0.000225	-1.01E-04	-6.42E-04	1.15E-04	-5.05E-05
a_4^{eq}	3.23209	0.015997	-0.105329	-0.018725	0.002379	-0.003153	0.003897	-0.000443	0.000244	-7.84E-05	-2.79E-04	3.82E-05	-2.06E-05
a_5^{eq}	3.412773	-0.011158	-0.09399	-0.004827	0.002356	-2.24E-03	0.000617	-0.000623	1.46E-04	-3.84E-05	-1.19E-05	3.66E-05	-3.67E-05
a_6^{eq}	3.506561	0.018226	-0.102517	-0.02345	0.006194	-0.002934	4.86E-03	-0.001432	6.05E-04	-7.96E-05	-3.46E-04	1.08E-04	-5.72E-05
a_7^{eq}	3.506037	0.000662	-0.097295	-0.017872	0.00285	-0.002919	0.004808	-0.000183	6.17E-04	-7.51E-05	-4.27E-04	8.78E-06	-3.07E-05
a_8^{eq}	2.14331	-0.000928	-0.119999	-0.005795	0.002536	-0.005078	1.39E-03	0.000209	2.93E-05	-1.36E-04	-0.000108	-2.71E-05	-4.82E-06
b_1^{eq}	8.185678	0.002758	0.05985	0.014419	0.001688	0.001762	-4.70E-03	-7.83E-05	5.58E-05	4.30E-05	4.34E-04	-1.54E-05	-9.05E-06
b_2^{eq}	8.869649	-0.029608	0.058091	0.005957	-0.001627	0.001486	-8.59E-04	0.000281	-8.09E-05	3.46E-05	5.13E-05	-3.39E-05	-6.57E-06
b_3^{eq}	9.604007	0.009	0.072687	-0.002042	0.00139	0.002126	0.000147	-0.000341	3.96E-05	5.06E-05	4.92E-06	1.75E-05	-1.67E-05
b_4^{eq}	10.31207	-0.010974	0.070462	0.005786	-0.00021	0.001827	-0.00126	3.72E-05	-2.44E-05	3.44E-05	9.09E-05	-7.28E-06	1.50E-06
b_5^{eq}	10.76373	-6.69E-03	0.06755	0.003914	0.000246	0.001925	-1.20E-03	-2.92E-04	-7.93E-05	4.45E-05	1.22E-04	3.83E-05	4.07E-06
b_6^{eq}	11.08908	0.010521	0.064075	-0.005576	0.002253	0.001883	0.000692	-0.000794	7.33E-05	4.34E-05	-2.40E-06	8.67E-05	-4.31E-06
b_7^{eq}	11.35902	-0.003179	0.0643	0.000868	0.000499	0.001791	-1.99E-04	-0.000105	3.21E-05	4.11E-05	1.58E-05	1.03E-05	9.71E-07
b_8^{eq}	11.71941	-0.000954	0.100886	-0.001549	2.59E-04	0.00645	7.09E-04	2.13E-05	5.01E-05	2.10E-04	-7.91E-05	-6.90E-06	-7.80E-06
c_1^{eq}	-1.39116	-0.143516	0.094047	0.009853	-0.010312	0.001449	0.004833	0.000999	-0.000667	-5.16E-05	-6.10E-04	-3.78E-05	4.79E-05
c_2^{eq}	-1.596411	-0.187092	0.054767	0.141901	-0.007228	-0.001475	-0.037177	0.004669	0.000588	-0.000139	3.23E-03	-5.96E-04	5.60E-06
c_3^{eq}	-1.547451	0.066859	0.063709	-0.025208	0.007269	0.002743	0.004076	-0.002569	-0.000272	9.58E-05	-2.28E-04	2.57E-04	1.90E-05
c_4^{eq}	-1.736177	-0.04716	0.047029	0.017783	-0.016571	0.001021	-0.002458	0.004972	-0.000898	-7.14E-06	6.98E-05	-4.15E-04	1.60E-04
c_5^{eq}	-1.878835	0.080386	0.044049	-0.038666	0.005369	0.002548	0.006026	-0.002326	-0.000166	9.20E-05	-2.34E-04	2.80E-04	1.95E-05
c_6^{eq}	-1.965198	-0.013076	0.034078	0.006134	0.002581	-0.000673	-0.000811	-9.27E-05	3.39E-04	-5.09E-05	7.59E-06	1.78E-05	2.91E-05
c_7^{eq}	-2.131654	0.394373	-0.001909	-0.264532	0.01199	-0.003503	0.066224	-0.005314	-4.40E-05	-0.000177	-0.005564	6.30E-04	7.24E-06
c_8^{eq}	-1.65582	-0.068852	0.082272	0.020623	-0.001633	4.78E-04	-0.001202	0.0018	7.33E-04	-0.000106	-1.01E-04	-2.24E-04	-4.79E-05
λ_1	1136593	162278.7	4919.263	-110923.4	8700.356	-739.1671	27501.84	-2420.642	563.6006	-58.36081	-2283.962	270.0947	-15.16192
λ_2	-55.03018	-0.340312	-1.206588	-4.652112	-1.127481	0.090793	1.5362	0.172984	-0.055993	0.003532	-0.148127	-0.010352	0.003772

Table A.2. Continued.

	M_t (kg/kmol)														
	ξ_{00}	ξ_{10}	ξ_{01}	ξ_{20}	ξ_{11}	ξ_{02}	ξ_{30}	ξ_{21}	ξ_{12}	ξ_{03}	ξ_{40}	ξ_{31}	ξ_{22}	ξ_{13}	
a_2^M	2.266963	-1.096096	-0.00123	0.274652	0.000149	-0.000236	-0.049081	0.000282	0.000132	-8.47E-06	0.003594	-6.94E-05	-1.16E-05	5.00E-06	
a_3^M	1.952006	-0.361525	-0.000424	0.058866	0.000428	1.37E-05	-0.007083	-0.000103	-8.02E-06	4.53E-07	3.93E-04	8.17E-06	-8.19E-07	-8.75E-07	
a_4^M	0.860893	-0.665758	-0.001402	0.100323	-0.001688	-4.65E-05	-0.012112	0.000394	1.11E-05	-6.33E-07	6.88E-04	-1.66E-05	1.54E-05	5.34E-06	
a_5^M	0.223394	-0.453833	0.004065	0.051948	0.000174	1.46E-04	-0.005189	-5.49E-05	2.46E-06	-4.52E-06	0.00026	3.92E-06	-7.20E-07	1.74E-07	
a_6^M	-0.348842	-0.356119	0.003212	0.036125	-0.000909	0.000266	-0.003732	0.000157	-5.25E-05	7.32E-06	2.11E-04	-5.94E-06	8.96E-06	2.05E-07	
a_7^M	-0.638468	-0.255556	0.000653	0.007127	0.001264	-0.000129	0.001732	-0.00061	-1.02E-05	-8.16E-06	-1.75E-04	8.45E-05	2.33E-06	-4.67E-07	
a_8^M	-2.52645	-0.153855	-0.005414	-0.021514	0.007352	-0.000151	0.004023	-0.002828	1.26E-05	-1.37E-05	-6.67E-05	3.33E-04	4.95E-06	2.77E-07	
b_1^M	8.195886	-0.093007	0.060415	0.073774	2.14E-05	0.00176	-0.019171	0.000454	2.97E-05	3.99E-05	0.00163	-6.28E-05	7.70E-07	7.93E-07	
b_2^M	8.823667	0.004928	0.057076	-0.010969	-0.000867	0.001424	0.00319	3.94E-05	-6.04E-05	2.70E-05	-2.85E-04	3.19E-06	1.84E-06	-1.82E-06	
b_3^M	9.543688	0.007416	0.071456	-0.001467	0.000837	0.002073	0.000139	-0.000143	1.26E-05	4.41E-05	-3.76E-06	9.93E-06	-1.08E-06	3.43E-08	
b_4^M	10.29095	0.006853	0.068933	-0.001976	5.13E-05	0.00178	0.000386	1.07E-05	-4.35E-06	3.41E-05	-3.05E-05	-1.12E-06	5.31E-07	-2.14E-07	
b_5^M	10.74839	-0.001804	0.064935	0.000328	-0.000475	0.001479	3.66E-05	1.32E-04	-9.45E-06	2.44E-05	-9.88E-06	-8.94E-06	3.74E-06	6.27E-07	
b_6^M	11.08649	-0.001236	0.062025	0.000507	0.000623	0.001417	-0.000169	-0.000108	6.86E-05	2.29E-05	1.46E-05	7.81E-07	-7.16E-06	1.70E-06	
b_7^M	11.38418	-0.042498	0.072513	0.017401	-0.009966	0.002303	-0.002689	0.00227	-6.96E-04	4.41E-05	1.42E-04	-1.34E-04	8.13E-05	-1.28E-05	
b_8^M	11.67614	-0.107179	0.067361	0.050281	-0.012522	0.002773	-0.009217	0.003612	-4.74E-04	0.000103	0.000578	-3.14E-04	5.95E-05	-5.90E-06	
c_1^M	2.474094	-0.375539	-0.073192	0.316855	-0.003339	-0.001935	-0.088337	0.002056	4.14E-05	-2.63E-05	7.90E-03	-2.46E-04	-5.79E-06	-6.65E-07	
c_2^M	2.455022	0.080699	-0.048362	-0.068114	0.000985	-0.000758	0.018978	-0.000135	4.51E-05	-8.30E-06	-0.001707	8.17E-06	-8.60E-06	-1.34E-06	
c_3^M	2.301124	-0.035348	-0.066133	0.011457	-0.000816	-0.001908	-0.001977	0.000224	1.39E-05	-3.94E-05	1.33E-04	-2.00E-05	6.87E-07	1.28E-06	
c_4^M	2.595419	0.032911	-0.048502	-0.00837	0.001987	-0.001769	0.001646	-0.000276	1.13E-04	-4.01E-05	-1.31E-04	1.56E-05	-5.02E-06	4.55E-06	
c_5^M	2.611683	0.00722	-0.047775	-0.007095	-0.002323	-1.15E-03	0.002062	0.000398	-0.000167	-7.77E-06	-0.000172	1.46E-05	3.49E-05	6.33E-07	
c_6^M	2.703058	0.027752	-0.052293	-0.025826	-0.007296	-0.00201	0.007507	0.000979	-6.81E-04	-8.67E-05	-0.000656	4.40E-05	9.27E-05	-8.63E-06	
c_7^M	2.646768	-0.070787	-0.059517	0.0409	-0.00632	-0.005176	-0.009092	0.00191	-0.000245	-0.000216	6.85E-04	-1.89E-04	2.53E-05	-3.52E-06	
c_8^M	2.672429	0.133919	-0.069491	-0.019029	0.03175	-0.001516	-0.0143	-0.014129	0.000213	-1.69E-05	0.002694	0.001664	-3.16E-05	6.88E-06	
a_1^M	1.368591	2.493734	-0.002591	-2.266136	0.006045	-3.62E-05	0.86761	-0.004278	4.14E-05	-0.153462	0.001101	-2.28E-05	0.010227	-9.39E-05	2.96E-06
λ_3	24.93886	9.344645	-0.000745	-14.97752	0.001263	-6.51E-05	6.456078	-7.67E-05	0.000129	-1.197114	-0.000104	-4.37E-05	0.081749	1.55E-05	4.21E-06

Table A.3. CH₄/air plasma.

	ξ_{00}	ξ_{10}	ξ_{01}	ξ_{20}	ξ_{02}	ξ_{21}	ξ_{12}	ξ_{03}	ξ_{22}	ξ_{13}	ξ_{04}	ξ_{23}	ξ_{14}	ξ_{05}
a_1^{off}	0.497235	-0.010146	0.006146	0.132319	-0.004705	-1.32E-04	0.003779	-0.000401	-0.002773	0.000293	-7.41E-06	-0.000171	4.80E-06	2.97E-08
a_2^{off}	-0.492009	0.063951	0.024955	-0.078895	0.003734	-0.00132	0.005689	-0.000704	-0.001277	-0.000208	-4.84E-05	1.82E-05	-2.40E-05	1.58E-08
a_3^{off}	0.136237	0.30128	0.001404	-0.062065	0.013145	0.004856	-0.00231	-0.003133	0.000619	-1.73E-04	2.66E-05	4.72E-05	-1.79E-06	9.90E-09
a_4^{off}	0.47622	0.009606	0.000554	-0.020947	-0.008987	7.70E-05	-0.001349	0.000153	-1.31E-04	1.17E-05	8.17E-06	-5.66E-06	1.79E-06	1.49E-08
a_5^{off}	0.458757	0.064372	-0.036187	0.024215	-2.26E-04	-0.010297	0.003277	-1.71E-05	-0.000196	0.000329	-4.02E-06	2.24E-05	1.37E-05	4.95E-09
a_6^{off}	0.042087	-0.479118	-0.001569	0.330713	-0.10352	0.081911	-0.008013	4.78E-05	0.004647	-7.12E-04	1.67E-05	2.07E-05	-3.79E-05	-3.17E-08
a_7^{off}	-0.271327	1.338115	-0.010471	-0.884048	0.233342	0.004274	-0.168054	0.005653	-0.000159	4.97E-04	-3.69E-05	0.000314	6.16E-05	-3.07E-08
a_8^{off}	-0.999978	-1.01828	0.045122	0.448092	-0.054759	-0.007118	0.019203	-0.000117	-0.008288	0.00084	5.80E-05	-0.000528	-9.81E-06	2.21E-06
b_1^{off}	4.883268	0.768414	-0.076613	-0.185001	0.068064	0.018553	-0.020469	0.004553	0.002715	-0.008897	1.02E-04	-0.000601	-4.57E-05	7.92E-09
b_2^{off}	8.911241	-0.007505	0.048443	0.003303	-0.001354	0.000606	-0.000434	0.000603	-0.0002	7.85E-05	-1.52E-05	4.24E-05	-7.02E-06	-1.09E-08
b_3^{off}	9.582611	0.006211	0.061922	-0.003823	-0.002991	0.000358	-0.000438	-0.000227	-4.85E-05	1.27E-04	-1.56E-06	7.02E-06	3.13E-06	-5.94E-09
b_4^{off}	10.31256	-0.005942	0.06253	0.000768	0.001855	0.000335	-0.000259	8.38E-06	-8.29E-05	-4.33E-05	-3.42E-06	-4.93E-07	-2.00E-06	4.95E-09
b_5^{off}	10.75312	-0.000119	0.067008	-0.002887	-0.002425	0.001812	0.000917	-3.54E-04	3.02E-05	2.64E-04	6.82E-06	-5.10E-07	1.33E-05	-8.91E-09
b_6^{off}	11.11139	-0.039429	0.065116	0.022776	-0.013731	0.002108	0.008991	-0.001642	6.94E-05	0.001096	1.00E-06	3.98E-05	-2.02E-07	-8.91E-09
b_7^{off}	11.36593	0.012699	0.057597	-0.010485	0.005624	-0.000397	-0.002071	0.001757	-2.00E-04	-0.000238	1.92E-04	-1.02E-05	6.28E-06	-1.34E-07
b_8^{off}	11.77548	-0.302768	0.09083	0.085835	-0.091709	0.002191	0.024234	-0.005771	-2.15E-05	0.001765	1.69E-05	3.23E-05	1.86E-05	1.18E-06
c_1^{off}	-0.876133	1.031048	-0.060732	-0.620664	0.053666	-0.013877	-0.005611	0.002462	0.002339	-5.60E-04	6.32E-05	8.08E-05	-2.37E-05	-2.67E-08
c_2^{off}	2.425062	-0.144835	-0.026844	0.052425	0.01215	-0.005304	0.002111	-0.007377	0.000853	0.002406	6.90E-05	6.77E-05	1.03E-05	1.68E-08
c_3^{off}	2.500415	-0.049854	-0.003852	0.024875	-0.007965	-0.008848	0.000644	0.001835	-0.002085	-0.00087	-9.87E-05	-3.34E-05	-2.23E-07	1.78E-08
c_4^{off}	2.602944	-0.01988	-0.043329	0.016452	0.015017	-0.002515	-0.000861	0.000504	-1.39E-06	-1.39E-04	4.55E-06	-4.68E-06	-1.12E-05	-2.93E-20
c_5^{off}	2.618781	-0.05165	-0.054351	0.032002	-0.006586	-0.002731	0.001594	-0.000101	-8.64E-04	-0.000215	-2.74E-06	-6.33E-05	-1.25E-05	1.88E-08
c_6^{off}	2.72428	0.297453	-0.024522	-0.225509	-0.032982	0.004284	0.00253	-3.87E-04	0.009669	-0.000112	-4.88E-05	0.000627	5.25E-05	-8.91E-09
c_7^{off}	2.680191	-0.391015	-0.126438	0.292187	0.07528	-0.0136	-0.02482	0.01997	0.000791	-0.014036	5.88E-05	-0.000799	-6.41E-05	3.87E-06
c_8^{off}	1.407622	3.445276	-0.266793	-1.881354	0.570463	-0.004332	-0.318174	0.011754	-0.000518	-0.000498	-0.000233	0.000618	4.80E-05	-3.57E-06

Table A.3. Continued.

	$c_{p,off}$ (kJ/kg K)	$c_{p,eq}$ (kJ/kg K)	h (kJ/kg)	s (kJ/kg K)
$a_{1,eq}$	1.170969	1.120215	-0.127371	-0.290187
$a_{2,eq}$	2.497633	-0.04266	-0.102196	0.001199
$a_{3,eq}$	2.924353	0.173386	-0.131045	-0.022048
$a_{4,eq}$	3.23299	0.011512	-0.101949	-0.013172
$a_{5,eq}$	3.40678	0.007096	-0.090306	-0.009632
$a_{6,eq}$	3.5286	-0.049264	-0.082688	0.008316
$a_{7,eq}$	3.493682	-0.019162	-0.089302	-0.013282
$a_{8,eq}$	2.221276	-0.051149	-0.110099	0.023218
$b_{1,eq}$	8.160764	0.009346	0.053899	0.004648
$b_{2,eq}$	8.864583	-0.011165	0.058248	-0.000784
$b_{3,eq}$	9.603162	0.003438	0.072201	0.000246
$b_{4,eq}$	10.31104	-0.004258	0.06884	-0.001763
$b_{5,eq}$	10.76042	-6.32E-06	0.064195	-0.000807
$b_{6,eq}$	11.09144	0.004937	0.059122	-0.004803
$b_{7,eq}$	11.36394	-0.01719	0.062897	0.007962
$b_{8,eq}$	11.74009	0.043901	0.156427	-0.019666
$c_{1,eq}$	-1.783352	0.805418	0.068536	-0.466204
$c_{2,eq}$	-1.576631	-0.214399	0.06253	0.138516
$c_{3,eq}$	-1.470337	-0.066531	0.056063	0.038827
$c_{4,eq}$	-1.706674	-0.059008	0.054224	0.028781
$c_{5,eq}$	-1.911221	0.169039	0.018469	-0.067678
$c_{6,eq}$	-1.885694	-0.150879	0.018103	0.06549
$c_{7,eq}$	-1.94994	-0.021065	0.048714	0.019304
$c_{8,eq}$	-1.68478	0.440727	0.126274	-0.230738
λ_1	1239204	60992.76	47304.83	-39281
λ_2	-54.8455	-6.450537	-1.453109	3.333452
				-2.885249
				0.039988
				1.890681
				-0.423165
				-0.012156
				0.281657
				-0.017091
				-0.001429
				0.01251
				0.000145
				-3.64E-05
				1.862041
				-2.774747
				46.37552
				-75.06363
				-347.3295
				492.5372
				-47.39907
				-0.017091
				-0.001429
				0.01251
				0.000145
				-3.64E-05
				1.862041
				-2.774747
				46.37552
				-75.06363
				-347.3295
				492.5372
				-47.39907
				-0.017091
				-0.001429
				0.01251
				0.000145
				-3.64E-05
				1.862041
				-2.774747
				46.37552
				-75.06363
				-347.3295
				492.5372
				-47.39907
				-0.017091
				-0.001429
				0.01251
				0.000145
				-3.64E-05
				1.862041
				-2.774747
				46.37552
				-75.06363
				-347.3295
				492.5372
				-47.39907
				-0.017091
				-0.001429
				0.01251
				0.000145
				-3.64E-05
				1.862041
				-2.774747
				46.37552
				-75.06363
				-347.3295
				492.5372
				-47.39907
				-0.017091
				-0.001429
				0.01251
				0.000145
				-3.64E-05
				1.862041
				-2.774747
				46.37552
				-75.06363
				-347.3295
				492.5372
				-47.39907
				-0.017091
				-0.001429
				0.01251
				0.000145
				-3.64E-05
				1.862041
				-2.774747
				46.37552
				-75.06363
				-347.3295
				492.5372
				-47.39907
				-0.017091
				-0.001429
				0.01251
				0.000145
				-3.64E-05
				1.862041
				-2.774747
				46.37552
				-75.06363
				-347.3295
				492.5372
				-47.39907
				-0.017091
				-0.001429
				0.01251
				0.000145
				-3.64E-05
				1.862041
				-2.774747
				46.37552
				-75.06363
				-347.3295
				492.5372
				-47.39907
				-0.017091
				-0.001429
				0.01251
				0.000145
				-3.64E-05
				1.862041
				-2.774747
				46.37552
				-75.06363
				-347.3295
				492.5372
				-47.39907
				-0.017091
				-0.001429
				0.01251
				0.000145
				-3.64E-05
				1.862041
				-2.774747
				46.37552
				-75.06363
				-347.3295
				492.5372
				-47.39907
				-0.017091
				-0.001429
				0.01251
				0.000145
				-3.64E-05
				1.862041
				-2.774747
				46.37552
				-75.06363
				-347.3295
				492.5372
				-47.39907
				-0.017091
				-0.001429
				0.01251
				0.000145
				-3.64E-05
				1.862041
				-2.774747
				46.37552
				-75.06363
				-347.3295
				492.5372
				-47.39907
				-0.017091
				-0.001429
				0.01251
				0.000145
				-3.64E-05
				1.862041
				-2.774747
				46.37552
				-75.06363
				-347.3295
				492.5372
				-47.39907
				-0.017091
				-0.001429
				0.01251
				0.000145
				-3.64E-05
				1.862041
				-2.774747
				46.37552
				-75.06363
				-347.3295
				492.5372
				-47.39907
				-0.017091
				-0.001429
				0.01251
				0.000145
				-3.64E-05
				1.862041
				-2.774747
				46.37552
				-75.06363
				-347.3295
				492.5372
				-47.39907
				-0.017091
				-0.001429
				0.01251
				0.000145
				-3.64E-05
				1.862041
				-2.774747
				46.37552
				-75.06363
				-347.3295
				492.5372
				-47.39907
				-0.017091
				-0.001429
				0.01251
				0.000145
				-3.64E-05
				1.862041
				-2.774747
				46.37552
				-75.06363
				-347.3295
				492.5372
				-47.39907
				-0.017091
				-0.001429
				0.01251
				0.000145
				-3.64E-05
				1.862041
				-2.774747
				46.37552
				-75.06363
				-347.3295
				492.5372
				-47.39907
				-0.017091
				-0.001429
				0.01251
				0.000145
				-3.64E-05
				1.862041
				-2.774747
				46.37552
				-75.06363
				-347.3295
				492.5372
				-47.39907
				-0.017091
				-0.001429
				0.01251
				0.000145
				-3.64E-05
				1.862041
				-2.774747
				46.37552
				-75.06363
				-347.3295
				492.5372
				-47.39907
				-0.017091
				-0.001429
				0.01251
				0.000145
				-3.64E-05
				1.862041
				-2.774747
				46.37552
				-75.06363
				-347.3295
				492.5372
				-47.39907
				-0.017091
				-0.001429
				0.01251
				0.000145
				-3.64E-05
				1.862041
				-2.774747
				46.37552
				-75.06363
				-347.3295
				492.5372
				-47.39907
				-0.017091
				-0.001429
				0.01251
				0.000145
				-3.64E-05
				1.862041
				-2.774747
				46.37552
				-75.06363
				-347.3295
				492.5372
				-47.39907
				-0.017091
				-0.001429
				0.01251
				0.000145
				-3.64E-05
				1.862041
				-2.774747
				46.37552
				-75.06363
				-347.3295

Table A.3. Continued.

	M_t (kg/kmol)													
	ξ_{00}	ξ_{10}	ξ_{01}	ξ_{20}	ξ_{11}	ξ_{02}	ξ_{30}	ξ_{21}	ξ_{12}	ξ_{03}	ξ_{40}	ξ_{31}	ξ_{22}	ξ_{13}
a_1^M	6.430346	-20.59475	-0.017419	35.11529	0.044612	-0.000621	-2.49E+01	-0.03549	0.001003	-7.65E-06	6.314178	8.50E-03	-0.000481	1.21E-06
a_2^M	0.779075	6.190502	0.026094	-11.17136	-0.067616	0.000817	7.919848	0.047522	-0.001904	-5.45E-06	-2.006626	-8.69E-03	1.04E-03	8.13E-06
a_3^M	2.088849	-0.834086	-0.004443	1.099449	0.013696	-1.81E-05	-0.772545	-0.010785	0.000183	4.29E-06	1.99E-01	2.74E-03	-1.19E-04	-3.00E-06
a_4^M	1.116831	-1.149791	0.034983	0.786855	-0.12332	1.10E-05	-0.167662	0.119168	-0.001175	-2.39E-05	-3.73E-02	-3.63E-02	7.07E-04	1.18E-05
a_5^M	-3.863098	16.34086	-0.164651	-23.84476	0.560625	-1.19E-03	14.62394	-0.585652	1.10E-03	-9.48E-05	-3.236748	1.96E-01	1.37E-04	7.46E-05
a_6^M	-0.416964	-0.0106	-0.009535	-0.2598	-0.055112	-0.005661	0.115142	0.000311	-6.48E-03	-0.000509	7.73E-03	2.54E-02	5.66E-03	2.30E-04
a_7^M	5.776032	-27.2272	0.116906	41.33618	-0.35928	0.000245	-27.22584	0.382244	0.002239	6.91E-05	6.54E+00	-1.34E-01	-0.001828	-4.60E-05
a_8^M	13.85832	-58.67581	1.188396	78.08012	-2.825995	0.037822	-45.97701	2.148978	-0.068526	-6.65E-06	10.12679	-5.17E-01	0.029907	-3.87E-05
b_1^M	7.444697	3.301052	0.061611	-5.526276	-0.008931	0.001712	3.898451	0.005058	-0.000182	3.80E-05	-0.983131	-4.80E-04	4.03E-05	-4.05E-06
b_2^M	9.025076	-0.916142	0.053798	1.511813	0.007276	0.001327	-1.063918	-0.005827	0.000139	2.71E-05	2.69E-01	1.10E-03	-1.04E-04	-2.37E-06
b_3^M	9.511017	0.144884	0.071576	-0.234187	0.00052	0.002108	0.160985	-0.000379	-9.20E-06	4.56E-05	-3.99E-02	1.94E-04	6.09E-06	-4.66E-07
b_4^M	10.3085	-0.057311	0.071718	0.049994	-0.009018	0.00182	-0.00862	8.97E-03	-1.07E-04	3.46E-05	-3.79E-03	-2.78E-03	4.71E-05	-1.17E-06
b_5^M	10.27879	1.961269	0.053431	-2.951855	0.037831	0.001387	1.896233	-4.22E-02	-2.16E-04	1.01E-05	-4.42E-01	1.51E-02	2.10E-04	1.03E-05
b_6^M	9.069924	8.464317	0.013068	-12.75324	0.154179	0.000207	8.213707	-0.173727	-9.82E-04	-9.69E-05	-1.92E+00	6.37E-02	1.22E-03	7.36E-05
b_7^M	9.371168	7.821829	-0.043865	-10.85418	0.332449	-0.000782	6.305907	-0.37113	-2.14E-03	-0.000184	-1.30E+00	1.33E-01	2.07E-03	9.99E-05
b_8^M	14.27568	-9.973113	0.20604	13.80429	-0.433682	0.001587	-8.447706	0.334434	-9.77E-03	-0.000242	1.929861	-7.85E-02	5.46E-03	1.14E-04
c_1^M	-5.088415	33.71181	-0.055369	-55.33903	-0.046527	-0.001838	38.7386	0.035283	-0.000213	-1.91E-05	-9.77E+00	-8.64E-03	6.75E-06	-2.36E-06
c_2^M	0.4049066	-7.209922	-0.063165	11.87222	0.041731	-0.000969	-8.333286	-0.030271	0.000294	-9.04E-06	2.105179	6.81E-03	-2.37E-04	-5.66E-06
c_3^M	2.106554	0.875651	-0.061822	-1.515111	-0.011044	-0.001861	1.078719	0.009621	-0.000308	-4.53E-05	-2.76E-01	-2.34E-03	1.37E-04	-1.23E-06
c_4^M	2.549737	-0.02525	-0.075129	0.430601	0.094872	-0.001649	-0.550828	-0.088378	8.70E-04	-9.93E-06	1.95E-01	2.63E-02	-6.33E-04	-1.76E-05
c_5^M	4.538237	-7.541132	0.06812	10.25639	-0.386149	-9.54E-05	-5.870282	0.393446	-0.002188	3.09E-05	1.193258	-1.28E-01	8.23E-04	-3.53E-05
c_6^M	-1.122953	15.04155	-0.261769	-20.71645	0.715889	-0.001494	11.94269	-0.754682	-6.12E-04	-6.70E-05	-2.441927	2.53E-01	2.62E-05	-1.82E-05
c_7^M	4.53999	-7.576703	0.063945	10.15983	-0.393544	0.000465	-5.50541	0.455627	0.002179	0.000287	1.00E+00	-1.73E-01	-0.004106	-3.14E-04
c_8^M	3.054484	-1.366852	-0.132466	2.481974	0.271218	-0.00386	-2.315441	-0.307614	0.005328	-8.13E-05	0.753935	0.099294	-0.00235	1.38E-04
λ_3	70.23199	-189.2254	-0.005767	309.2387	0.02949	0.000516	-217.1366	-0.045316	-0.001592	-1.83E-05	54.62963	0.021279	0.001129	2.35E-05

References

- O. Askari, S.K. Hannani, R. Ebrahimi, J. Mech. Sci. Technol. **26**, 1205 (2012)
- F.R. Gilmore, Equilibrium Composition and Thermodynamic Properties of Air to 24 000° K, U.S. Air Force, The Rand Corporation, Report No. RM-1543, 1955
- F.R. Gilmore, Additional Values for the Equilibrium Composition and Thermodynamic Properties of Air, U.S. Air Force, The RAND Corporation, Report No. RM-2328, 1959
- C.F. Hansen, S.P. Heims, A review of the thermodynamic, transport and chemical reaction rate properties of high temperature air, National Advisory Committee for Aeronautics (NACA), Report No. TN-4359, 1958
- C.F. Hansen, Thermodynamic and transport properties of high temperature air, Advisory Group for Aeronautical Research and Development, Report No. 323, 1959
- C.F. Hansen, Approximation for the thermodynamic and transport properties of high temperature air, National Aeronautics and Space Administration (NASA), Report No. R-50, 1960
- B.M. Rosenbaum, L. Levitt, Thermodynamic Properties of Hydrogen from Room Temperature to 100 000 K, National Aeronautics and Space Administration (NASA), Report No. TN-1107, 1962
- W.J. Lick, H.W. Emmons, *Thermodynamic Properties of Helium to 50 000 K* (Harvard University Press, Cambridge, Massachusetts, 1962)
- W.G. Browne, Thermodynamic Properties of the Earth's Atmosphere, Radiation and Space Phys. Tech. Mem. No. 2, Missile and Space Div., Gen. Elec. Co., 1962
- W.G. Browne, Equilibrium Thermodynamic Properties of the Environment of Mars, Advanced Aerospace Phys. Tech. Mem. No. 2, Missile and Space Vehicle Dept., Gen. Elec. Co., 1962
- W.G. Browne, Thermodynamic Properties of the Venusian Atmosphere - Part 1, Advanced Aerospace Phys. Tech. Mem. No. 13, pt. 1, Missile and Space Vehicle Dept., Gen. Elec. Co., 1962
- K.S. Drellishak, C.F. Knopp, A.B. Cambel, Phys. Fluids **6**, 1280 (1963)
- R.F. Kubin, L.L. Presley, Thermodynamic Properties and Mollier Chart for Hydrogen from 300 K to 20 000 K, National Aeronautics and Space Administration (NASA), Report No. SP-3002, 1964
- R.W. Patch, B.J. McBride, Partition functions and thermodynamic properties to high temperatures for H^{+3} and H^{+2} , National Aeronautics and Space Administration (NASA), Report No. D-4523, 1958
- R.W. Patch, Components of a hydrogen plasma including minor species, National Aeronautics and Space Administration (NASA), Report No. D-4993, 1969
- F. Nelson, Thermodynamic properties of hydrogen-helium plasmas, NASA CR-1861, 1971
- B. Pateyron, M.F. Elchinger, G. Delluc, P. Fauchais, Plasma Chem. Plasma Process. **12**, 421 (1992)
- S. Janisson, A. Vardelle, J.F. Coudert, E. Meillot, B. Pateyron, P. Fauchais, J. Thermal Spray Technol. **8**, 545 (1999)
- E. Sher, J. Ben-ya'ish, T. Kravchik, Combustion and Flame **89**, 186 (1992)
- M. Capitelli, G. Colonna, C. Gorse, Mol. Phys. Hypersonic Flows **482**, 293 (1995)
- M. Capitelli, G. Colonna, C. Gorse, Eur. Phys. J. D **11**, 279 (2000)
- D. Bruno, M. Capitelli, C. Catalfamo, D. Giordano, Phys. Plasmas **18**, 012308 (2011)
- M. Capitelli, S. Longo, G. Petrella, D. Giordano, Plasma Chem. Plasma Process. **25**, 659 (2005)
- M. Capitelli, G. Colonna, A. D'Angola, Pulsed Power Plasma Sci. **1**, 694 (2001)
- A. D'Angola, G. Colonna, C. Gorse, M. Capitelli, Eur. Phys. J. D **46**, 129 (2007)
- V. Rat, P. André, J. Aubreton, M.F. Elchinger, P. Fauchais, A. Lefort, Phys. Rev. E **64**, 026409 (2001)
- A.B. Murphy, Plasma Chem. Plasma Process. **20**, 279 (2000)
- A.B. Murphy, IEEE Trans. Plasma Sci. **25**, 809 (1997)
- O. Askari, H. Metghalchi, S. Kazemzadeh Hannani, A. Moghaddas, R. Ebrahimi, H. Hemmati, J. Energy Resour. Technol. **135**, 021001 (2012)
- O. Askari, H. Metghalchi, S. Kazemzadeh Hannani, H. Hemmati, R. Ebrahimi, J. Energy Resour. Technol. **136**, 022202 (2014)
- S. Gordon, B.J. McBride, Thermodynamic Data to 20 000 K for Monatomic Gases, National Aeronautics and Space Administration (NASA), Glenn Research Center, Report No. TP-1999-208523, 1999
- H.R. Griem, Phys. Rev. **128**, 997 (1962)
- W.B. White, S.M. Johnson, G.B. Dantzig, J. Chem. Phys. **28**, 751 (1958)
- S. Gordon, B.J. McBride, Computer program for calculation of complex chemical equilibrium compositions and applications. Part 1: Analysis, National Aeronautics and Space Administration (NASA), Report No. RP-1311, 1994
- K. Eisazadeh-Far, F. Parsinejad, H. Metghalchi, J.C. Keck, Combustion and Flame **157**, 2211 (2010)
- K. Eisazadeh-Far, H. Metghalchi, J.C. Keck, J. Energy Resour. Technol. **133**, 022201 (2011)
- E. Rokni, A. Moghaddas, O. Askari, H. Metghalchi, J. Energy Resour. Technol. **137**, 012204 (2014)
- O. Askari, A. Moghaddas, A. Alholm, K. Vein, B. Alhazmi, H. Metghalchi, Combustion and Flames **168**, 20 (2016)
- O. Askari, M. Janbozorgi, R. Greig, A. Moghaddas, H. Metghalchi, Sci. Technol. Built Environ. **21**, 220 (2015)
- O. Askari, K. Vien, Z. Wang, M. Sirio, H. Metghalchi, J. Appl. Energy (2016)
- F.T. Mackenzie, J.A. Mackenzie, *Our Changing Planet: An Introduction to Earth System Science and Global Environmental Change*, 4th edn. (Prentice Hall, 2010)
- E.P. Gyftopoulos, G.P. Beretta, *Thermodynamics: Foundations and Applications* (Dover Publications, Mineola, NY, 2005)
- J.A. Fay, *Molecular thermodynamic* (Addison-Wesley, Massachusetts, 1965)
- H.N. Olsen, Phys. Rev. **124**, 1703 (1961)
- Mc M. Chesney, Can. J. Phys. **42**, 2473 (1964)
- L.V. Gurvich, I.V. Veyts, C.B. Alcock, *Thermodynamic properties of individual substances* (Hemisphere Publishing Corporation, New York, 1989)
- M.W. Zemansky, *Heat and Thermodynamics: An Intermediate Textbook for Students of Physics, Chemistry, and Engineering*, 4th edn. (McGraw-Hill, New York, 1957)
- H. Myers, J.H. Buss, S.W. Benson, Planetary Space Science **3**, 257 (1961)

49. H.R. Griem, *Principle of Plasma Spectroscopy* (McGraw-Hill, 1964)
50. C.E. Moore, Atomic energy levels, U.S. Department of Commerce, National Bureau of Standards, NSRDS-NBS 35, Vol. 1. (1971)
51. H.G. Kuhn, *Atomic Spectra* (Academic Press, New York, 1962)
52. J. Cooper, Rep. Prog. Phys. **35**, 34 (1966)
53. Y.B. Zel'dovich, Y.P. Raizer, W.D. Hayes, R.F. Probststein, *Physics of shock waves and high temperature hydrodynamics phenomena* (Academic Press, New York and London, 1966)
54. J. Hilsenrath, M. Klein, Tables of Thermodynamic Properties of Air in Chemical Equilibrium Including Second Virial Corrections From 1500 K to 150 000 K, AEDC-TR-65-58, U.S. Air Force, Mar. 1965
55. M. Capitelli, E.F. Varracchio, Rev. Int. Htes Temp. Refract. **14**, 195 (1977)
56. R.M. Sevast'yanov, R.A. Chernyavskaya, J. Eng. Phys. **51**, 851 (1986)
57. Y. Cressault, A. Gleizes, G. Riquel, J. Phys. D **45**, 265202 (2012)
58. B. Bottin, Progress Aerospace Sci. **36**, 547 (2000)